Brain Tumor Pathol
DOI 10.1007/s10014-012-0113-1

ORIGINAL ARTICLE

Histopathological malignant progression of grade II and III gliomas correlated with *IDH1/2* mutation status

Makoto Ohno · Yoshitaka Narita · Yasuji Miyakita · Yoshiko Okita · Yuko Matsushita · Akihiko Yoshida · Shintaro Fukushima · Koichi Ichimura · Takamasa Kayama · Soichiro Shibui

Received: 1 April 2012 / Accepted: 21 June 2012

Abstract The impact of isocitrate dehydrogenase (*IDH1/2*) mutations on the malignant progression of gliomas was investigated by comparing the histopathological features of 53 grade II and III gliomas after recurrence according to the *IDH1/2* status. We identified *IDH1/2* mutations in 44.4 % (16 of 36) of astrocytic tumors and 70.6 % (12 of 17) of oligodendroglial tumors. Histopathological malignant progression was observed in 68.8 % (11 in 16) and 55 % (11 in 20) of astrocytic tumors with and without *IDH1/2* mutations, respectively. There were 8 secondary glioblastomas (GBM) that had progressed from 5 diffuse astrocytomas (DA) and 3 anaplastic astrocytomas (AA) with *IDH1/2* mutations. Seven secondary GBMs were derived from 3 DAs and 4 AAs with wild-type *IDH1/2*. Malignant progression was observed in 47.1 % (8 of 17) of oligodendroglial tumors. All 12 oligodendroglial tumors with *IDH1/2* mutations remained as such without progressing to GBM, whereas 3 of the 5 oligodendroglial tumors without *IDH1/2* mutations progressed to GBM at recurrence. In conclusion, grade II and III gliomas developed to more malignant histological types, irrespective of the *IDH1/2* mutation status, and the monitoring of the *IDH1/2* status could be of value to predict the development of GBM in patients with oligodendroglial tumors.

Keywords Astrocytoma · Oligodendroglioma · Glioblastoma · IDH · Malignant progression

M. Ohno · Y. Narita (✉) · Y. Miyakita · Y. Okita · Y. Matsushita · T. Kayama · S. Shibui
Department of Neurosurgery and Neuro-Oncology, National Cancer Center Hospital, 5-1-1, Tsukiji, Chuo-ku, Tokyo 104-0045, Japan
e-mail: yonarita@ncc.go.jp

A. Yoshida · S. Fukushima
Department of Pathology and Clinical Laboratories, National Cancer Center Hospital, 5-1-1, Tsukiji, Chuo-ku, Tokyo 104-0045, Japan

K. Ichimura
Division of Brain Tumor Translational Research, National Cancer Center Research Institute, 5-1-1, Tsukiji, Chuo-ku, Tokyo 104-0045, Japan

Introduction

According to the 2007 World Health Organization (WHO) classification, most gliomas are classified as astrocytoma, oligoastrocytoma, or oligodendroglioma [1]. Because of their tendency to diffusely infiltrate brain tissue and their resistance to radiation therapy and chemotherapy, these tumors often recur after surgical treatment and additional therapy [2]. Diffuse astrocytomas (DA: WHO grade II) and anaplastic astrocytomas (AA: WHO grade III) tend to progress to more malignant histological types and ultimately to secondary glioblastomas (GBM: WHO grade IV), whereas oligodendrogliomas (OL: WHO grade II) and oligoastrocytomas (OA: WHO grade II) progress to anaplastic oligodendrogliomas (AO: WHO grade III) or anaplastic oligoastrocytomas (AOA: grade III) [1, 3]. However, the grading of oligodendroglial tumors is still subjective, remaining considerably less reproducible than that of astrocytic tumors, and the existence of a grade IV variant is controversial [4]. It is also unclear whether oligodendroglial tumors can progress to GBM or GBM with oligodendroglial components at tumor recurrence.

Genetically, 70–80 % of grade II and III gliomas and secondary GBM harbor isocitrate dehydrogenase (*IDH1/2*) mutations, whereas most primary GBMs and a subset of low-grade gliomas lack the *IDH1/2* mutation [5–9]. In

Published online: 13 July 2012

addition, DA frequently carry both *IDH1/2* mutations and TP53 mutations, OL *IDH1/2* mutations and loss of 1p/19q, and OA *IDH1/2* mutations plus either TP53 mutations or loss of 1p/19q [10]. This has led to the idea that the majority of DA and OL are thought to originate from common glial precursor cells carrying *IDH1/2* mutations, and the addition of TP53 mutations or loss of 1p/19q in cells with *IDH1/2* mutations may favor the acquisition of the astrocytic or oligodendroglial phenotype [3], and progress to anaplastic gliomas as well as to secondary GBM [7].

The isocitrate dehydrogenase enzymes convert isocitrate to alpha-ketoglutarate and reduce NADP+ to NADPH. Loss of a wild-type *IDH1* or *IDH2* allele could lead to depletion of alpha-ketoglutarate and NADPH, which normally help to defend the cell against oxidative stress. Mutated IDH acquires a neomorphic activity to reduce alpha-ketoglutarate to D-2-hydroxyglutarate (D-2HG), in an NADPH-dependent manner. More than 60 different dioxygenases are present in cells, and they require alpha-ketoglutarate as a cofactor. D-2HG has a structure similar to that of alpha-ketoglutarate and competitively inhibits enzymatic activity of various dioxygenases, which may contribute to the pathogenesis of gliomas [11]. Grades II and III astrocytomas and secondary glioblastomas frequently harbor *IDH1/2* mutations and later develop missense mutations in *TP53* and other genes, supporting the idea that early *IDH1/2* mutations could promote later advantageous mutations that underlie the formation and progression of these tumors [12].

In this study, we reviewed the histopathological changes of tumors initially diagnosed as grade II or III gliomas that later recurred and evaluated the impact of *IDH1/2* mutations on malignant progression. Grade II and III astrocytomas developed to more malignant histological tumor types and eventually to GBM, irrespective of the *IDH1/2* mutation status. However oligodendroglial tumors with *IDH1/2* mutations never progressed to GBM.

Patients and methods

Patient characteristics

A total of 53 patients who were initially diagnosed with WHO grade II or III glioma and underwent 2 or more operations during the course of their illness at the National Cancer Center Hospital, Tokyo, Japan, from January 1990 to June 2010 were included in the study. All tumor samples obtained at the first, second, and subsequent surgeries if performed, were diagnosed by neuropathologists at our hospital according to the WHO classification scheme. Patients who were initially treated elsewhere and referred to our hospital for further treatment at the time of recurrence were eligible when tumor tissues from the initial operation could be obtained and the diagnosis was confirmed by our neuropathologists.

The clinical and operative records were reviewed. The following data were collected for each patient: clinical history; date of initial, second, and subsequent operations; postoperative adjuvant therapy; date of death or last hospital visit; tumor histopathology at each operation; and extent of resection. The definition of the extent of resection was based on the surgeon's operative notes and postoperative imaging studies in this analysis. Time to malignant progression was calculated from the date of initial operation to the date of subsequent operation in which the higher grade of the tumor was confirmed. This study was approved by the internal review board of the National Cancer Center.

IDH1/2 sequence analysis

Nucleic acid was extracted from paraffin-embedded specimens or frozen tissue samples using a DNeasy Blood & Tissue Kit (Qiagen, Maryland, USA), according to the manufacturer's protocol. A 129-bp fragment of IDH1 including codon 132 or a 150-bp fragment of IDH2 including codon 172 was amplified by PCR assay using the forward primer IDH1f: CGGTCTTCAGAGAAGCCATT and reverse primer IDH1r: GCAAAATCACATTATTGCCAAC, and the forward primer IDH2f: AGCCCATCATCTGCAAAAAC and reverse primer IDH2r: CTAGGCGAGGAGCTCCAGT. Thermocycling conditions consisted of 5 min at 95 °C, 35 cycles of 30 s at 95 °C, 40 s at 56 °C, and 50 s at 72 °C, followed by 10 min at 72 °C [6]. After purification of the PCR products with the QIAquick PCR Purification Kit (Qiagen, Maryland, USA), DNA sequencing of the *IDH* gene was performed with an ABI PRISM 310 Genetic Analyzer (Applied Biosystems) using the same primers.

IDH1 immunohistochemistry

Sections obtained from the paraffin block were immunostained with a mouse monoclonal anti-human IDH1 R132H antibody (Dianova, Hamburg, Germany; 1:20 dilution) according to the manufacturer's protocol. A strong cytoplasmic immunoreaction was scored as positive. Weak diffuse staining and staining of macrophages were scored as negative [13].

Statistical analysis

The χ^2 test or Fisher's exact test were used for comparisons of the frequency of malignant progression between mutated and wild-type *IDH1/2* tumors. Time to malignant progression was calculated according to the Kaplan–Meier method, and malignant progression and death were defined

Table 1 Patients characteristics of astrocytic tumors with and without IDH1/2 mutations

Case	Age (years)	Sex	Histology change	Time to malignant progression (months)	Survival (months)	Outcome	Tumor location	Surgery at initial treatment	Radiotherapy at initial treatment	Chemotherapy at initial treatment	IDH	IDH analysis
DA084	22	F	DA → DA		120.6	Alive	Rt. frontal	B	54 Gy	ACNU	Mut	IHC
DA038	30	F	DA → DA		114.0	Alive	Lt. frontal	TS	None	None	Mut	Seq
DA018	32	F	DA → AA → N	26.6	170.3	Alive	Lt. temporal	P	None	None	Mut	IHC
DA094	24	F	DA → GBM	69.3	74.8	Death	Rt. frontal	TS	60 Gy	ACNU	Mut	Seq
DA093	33	M	DA → AA → GBM	53.4	62.2	Alive	Rt. frontal	TS	None	None	Mut	IHC
DA082	50	M	DA → GBM	124	139.1	Alive	Rt. frontal	B	60 Gy	ACNU	Mut	Seq
DA021	21	M	DA → AOA	118.9	157.2	Alive	Rt. temporo-parietal	TS	None	None	Mut	Seq
DA083	26	F	DA → AOA	113.5	134.0	Alive	Rt. frontal	TS	52 Gy	ACNU	Mut	Seq
DA042	26	M	DA → AOA → GBM	70.7	76.9	Death	Lt. frontal	B	60 Gy	ACNU	Mut	Seq
DA027	41	M	DA → N		116.7	Death	Lt. frontal	P	60 Gy	ACNU	Mut	IHC
DA030	31	F	DA → N → DA → GBM	45.2	61.8	Death	Rt. fronto-temporal	P	50 Gy	None	Mut	Seq
AA052	34	F	AA → AO → AO → AO		78.6	Alive	Lt. frontal	P	Cyberknife	ACNU, CBDCA, VCR, Interferon	Mut	Seq
AA083	29	M	AA → GBM	16.1	18.6	Alive	Rt. frontal	P	60 Gy	TMZ	Mut	IHC
AA015	30	F	AA → GBM	31.7	34.2	Death	Lt. insula	B	60 Gy	ACNU, VP16	Mut	IHC
AA048	27	M	AA → GBM → GBM	45.3	52.5	Death	Rt. frontal	P	Dose unknown	ACNU, Interferon	Mut	IHC
AA010	43	M	AA → N		136.6	Death	Rt. parietal	TS	60 Gy	ACNU, VP16	Mut	Seq
DA064	72	F	DA → DA		37.5	Death (Sudden death)	Lt. temporal	B	54 Gy	None	Wt	Seq
DA047	29	F	DA → DA		77.0	Alive	Rt. thalamus	P	54 Gy	ACNU	Wt	IHC
DA098	34	F	DA → OA		105.3	Alive	Rt. fronto-temporal	B	None	None	Wt	Seq
DA011	32	M	DA → AA	107.3	121.2	Death	Lt. temporal	B	60 Gy	None	Wt	Seq
DA020	42	F	DA → AA	6.9	21.6	Death	Midbrain	P	60 Gy	ACNU	Wt	Seq
DA017	21	F	DA → AA	128.9	179.9	Alive	Rt. frontal	TS	None	None	Wt	Seq
DA086	36	M	DA → AA	83.8	88.4	Unknown	Rt. insula	P	50 Gy	None	Wt	IHC
DA085	30	M	DA → GBM → GBM	86.4	96.7	Death	Rt. temporal	TS	60 Gy	ACNU	Wt	Seq
DA048	28	M	DA → GBM	9.9	16.5	Death	Hypothalamus	B	50 Gy	ACNU	Wt	Seq
DA065	37	F	DA → GBM	15.2	21.5	Death	Rt. temporal-frontal	P	54 Gy	ACNU	Wt	Seq
DA036	58	M	DA → N		46.9	Death	Rt. frontal	TS	60 Gy	ACNU	Wt	Seq
DA024	53	M	DA → N		135.5	Unknown	Rt. frontal	P	60 Gy	ACNU	Wt	IHC

Table 1 continued

Case	Age (years)	Sex	Histology change	Time to malignant progression (months)	Survival (months)	Outcome	Tumor location	Surgery at initial treatment	Radiotherapy at initial treatment	Chemotherapy at initial treatment	IDH	IDH analysis
AA053	12	F	AA → DA		66.2	Unknown	Rt. temporal	TS	60 Gy	ACNU	Wt	Seq
AA008	37	M	AA → AA		55.3	Death	Lt. temporal	P	60 Gy	ACNU, VP16	Wt	IHC
AA042	61	F	AA → AA		27.1	Death	Rt. insular	P	60 Gy	ACNU	Wt	IHC
AA020	26	M	AA → AA → GBM	22.6	29.0	Death	Rt. frontal	TS	63 Gy	ACNU, VCR	Wt	Seq
AA009	42	M	AA → GBM	11.4	18.0	Death	Rt. frontal	P	60 Gy	ACNU, VP16	Wt	IHC
AA017	64	F	AA → GBM	12.6	36.7	Death	Rt. parietal	P	56 Gy	None	Wt	Seq
AA043	64	M	AA → GBM → GBM	7.2	14.0	Death	Rt. temporal	P	None	None	Wt	Seq
AA081	61	F	AA → N		15.8	Death	Lt. parietal	B	60 Gy	TMZ	Wt	IHC

M Male, *F* female, *DA* diffuse astrocytoma, *AA* anaplastic astrocytoma, *GBM* glioblastoma, *OL* oligodendroglioma, *OA* oligoastrocytoma, *AO* anaplastic oligodendroglioma, *AOA* anaplastic oligoastrocytoma, *N* necrosis, *Rt.* right, *Lt.* left, *B* biopsy, *P* partial removal, *TS* total or subtotal removal, *IDH* isocitrate dehydrogenase, *Mut* mutation, *Wt* wild-type, *ACNU* nimustine, *TMZ* temozolomide, *VP16* etoposide, *VCR* vincristine, *PCZ* procarbazine, *CBDCA* carboplatin, *IHC* immunohistochemistry, *Seq* sequence analysis

as events; differences were compared with the log-rank test. All analyses were conducted using JMP 7® software (SAS Institute Inc., Cary, NC, USA). In all cases, probability values <0.05 were considered statistically significant.

Results

Patient population and *IDH1/2* mutation

The characteristics of patients with astrocytic and oligodendroglial tumors are summarized in Tables 1 and 2. Fifty-three patients were analyzed, including 29 men and 24 women with a median age of 36 (range 12–72 years). The initial histology consisted of 23 DAs, 13 AAs, 7 OAs, 4 AOAs, 2 OLs, and 4 AOs. With regard to the extent of initial resection, there were 20 total or subtotal resections, 18 partial resections, 14 biopsies, and 1 unknown. After the initial operation, 35 patients received chemo-radiation therapy with nimustine hydrochloride (ACNU) or TMZ, 7 had radiation therapy alone, 2 had chemotherapy alone, and 9 had no adjuvant therapy.

IDH1/2 mutations, which were observed in the tumors of 28 patients, were detected by sequence analysis in 15 patients and by IHC in 13 patients. Three patients had tumors harboring mutations in *IDH2*. *IDH1/2* mutations were not observed in the tumors of 25 patients. Eighteen samples were confirmed by sequence analysis, and the remaining seven samples were negative for anti-IDH1 R132H antibody in IHC [13]. For these seven patients, frozen tissue or paraffin-fixed specimens were not available or suitable for direct sequence, and further screening for *IDH1* mutations other than the R132H and IDH2 mutations was not possible. Because the possibility of *IDH* mutations other than the R132H IDH1 mutation was reported to be less than 10 % [6, 12], we considered that the chances of these tumors having IDH mutations other than R132H are low and therefore combined these IHC-negative cases with sequence-confirmed *IDH1/2* wild-type cases, and classified them as tumors without *IDH1/2* mutation or *IDH1/2* wild-type tumors for further analyses.

Histopathological alterations

Astrocytic tumors

IDH1/2 mutations were observed in 44.4 % (16 of 36) astrocytic tumors. Malignant progression was observed in 61.1 % (22 of 36) astrocytic tumors; 68.8 % (11 of 16) were astrocytic tumors with *IDH1/2* mutations, and 55 % (11 of 20) were wild-type *IDH1/2*. Of 11 cases of *IDH1/2* mutated DA, 1 (9.1 %) developed to AA and 5 (45.5 %) to GBM; of these, 2 directly progressed to GBM, and the

Table 2 Patients characteristics of oligodendroglial tumors with and without IDH1/2 mutations

Case	Age (years)	Sex	Histology change	Time to malignant progression (months)	Survival (months)	Outcome	Tumor location	Surgery at initial treatment	Radiotherapy at initial treatment	Chemotherapy at initial treatment	IDH	IDH analysis
OL004	41	M	OL → AO → N	123.8	198.7	Death	Lt. parieto-occipital	B	None	ACNU, VCR	Mut	Seq
OA002	47	F	OA → OL		221.8	Death	Rt. frontal	TS	60 Gy	ACNU, PCZ, VCR	Mut	IHC
OA009	27	F	OA → OA		125.6	Death	Lt. frontal	B	None	None	Mut	IHC
OA023	43	M	OA → OA		102.9	Alive	Rt. frontal	TS	60 Gy	ACNU, VCR	Mut	IHC
OA010	27	M	OA → OA		91.7	Death	Lt. frontal	B	60 Gy	None	Mut	IHC
OA028	24	M	OA → AO	88.9	91.2	Alive	Lt. frontal	TS	60 Gy	ACNU, VCR	Mut	IHC
OA006	51	F	OA → AO	102.2	141.7	Death	Bifrontal	P	None	ACNU, PCZ, VCR	Mut	IHC
OA020	53	M	OA → AOA	7.9	109.5	Alive	Rt. parietal	P	None	None	Mut	Seq
AO013	52	F	AO → AO		83.4	Death (GIST)	Rt. parietal	TS	Dose unknown	ACNU, VCR	Mut	Seq
AO027	39	M	AO → AO → AO → AO → AO		51.7	Death	Rt. frontal	TS	60 Gy	TMZ	Mut	Seq
AOA020	28	M	AOA → AO		79.3	Alive	Rt. frontal	TS	60 Gy	ACNU, PCZ, VCR	Mut	Seq
AOA038	60	F	AOA → AOA		75.2	Death	Lt. frontal	TS	60 Gy	ACNU, PCZ, VCR	Mut	Seq
OL034	59	M	OL → AOA	4.7	19.2	Death (Pneumoniae)	Rt. frontal	B	60 Gy	None	Wt	Seq
AO001	36	M	AO → AO → AO → AO		100.3	Death	Lt. parieto-occipital	TS	70 Gy	ACNU, VP16	Wt	Seq
AO004	20	M	AO → GBM	9.8	16.0	Death	Rt. frontal	P	60 Gy	ACNU, VCR, PCZ	Wt	Seq
AOA010	62	M	AOA → GBM	14.2	31.8	Death	Rt. parietal	TS	60 Gy	ACNU, VCR	Wt	Seq
AOA025	47	F	AOA → AOA → GBM	29.1	35.9	Death	Rt. fronto-parietal	B	60 Gy	ACNU, VCR	Wt	Seq

M Male, *F* female, *DA* diffuse astrocytoma, *AA* anaplastic astrocytoma, *GBM* glioblastoma, *OL* oligodendroglioma, *OA* oligoastrocytoma, *AO* anaplastic oligodendroglioma, *AOA* anaplastic oligoastrocytoma, *N* necrosis, *Rt.* right, *Lt.* left, *B* biopsy, *P* partial removal, *TS* total or subtotal removal, *IDH* isocitrate dehydrogenase, *Mut* mutation, *Wt* wild-type, *ACNU* nimustine, *TMZ* temozolomide, *VP16* etoposide, *VCR* vincristine, *PCZ* procarbazine, *CBDCA* carboplatin, *IHC* immunohistochemistry, *Seq* sequence analysis, *GIST* gastrointestinal stromal tumor

Table 3 Summary of histopathological change of astrocytic and oligodendroglial tumors according to the IDH1/2 status

	n	DA (%)	AA (%)	GBM (%)	OL/OA (%)	AO/AOA (%)	Necrosis (%)	Malignant progression (%)
DA								
Mutation	11	2 (18.2 %)	1 (9.1 %)	5 (45.5 %)	0	2 (18.2 %)	1 (9.1 %)	8 (72.7 %)
Wild type	12	2 (16.7 %)	4 (33.3 %)	3 (25 %)	1 (8.3 %)	0	2 (16.7 %)	7 (58.3 %)
Total	23	4 (17.4 %)	5 (21.7 %)	8 (34.8 %)	1 (4.3 %)	2 (8.7 %)	3 (13.0 %)	15 (65.2 %)
AA								
Mutation	5	0	0	3 (60 %)	0	1 (20 %)	1 (20 %)	3 (60 %)
Wild type	8	1 (12.5 %)	2 (25 %)	4 (50 %)	0	0	1 (12.5 %)	4 (50 %)
Total	13	1 (7.7 %)	2 (15.4 %)	7 (53.8 %)	0	1 (7.7 %)	2 (15.4 %)	7 (53.8 %)
OL/OA								
Mutation	8	0	0	0	4 (50.0 %)	4 (50.0 %)	0	4 (50 %)
Wild type	1	0	0	0	0	1 (100 %)	0	1 (100 %)
Total	9	0	0	0	4 (44.4 %)	5 (55.6 %)	0	5 (55.6 %)
AO/AOA								
Mutation	4	0	0	0	0	4(100 %)	0	0 (0 %)
Wild type	4	0	0	3 (75 %)	0	1 (25 %)	0	3 (75 %)
Total	8	0	0	3 (37.5 %)	0	5 (62.5 %)	0	3 (37.5 %)

DA Diffuse astrocytoma, *AA* anaplastic astrocytoma, *GBM* glioblastoma, *OL* oligodendroglioma, *OA* oligoastrocytoma, *AO* anaplastic oligodendroglioma, *AOA* anaplastic oligoastrocytoma

other 3 ultimately progressed to GBM after multiple tumor recurrences. Two patients (18.2 %) with *IDH1/2* mutated DA were diagnosed with AOA and one patient with necrosis (9.1 %) at recurrence. Of 12 patients with wild-type *IDH1/2* DA, four progressed to AA (33.3 %) and three progressed directly to GBM (25 %). One patient with wild-type *IDH1/2* DA (8.3 %) was diagnosed with OA and two patients with necrosis (16.7 %) at recurrence. Of five patients with *IDH1/2* mutated AA, three (60 %) progressed to GBM. One patient with *IDH1/2* mutated AA had three recurrences and was diagnosed with AO each time (20 %). Of eight patients with wild-type *IDH1/2* AA, four (50 %) progressed to GBM. One patient was diagnosed with necrosis (12.5 %) at recurrence (Table 3).

The frequency of malignant progression did not differ between DA with and without *IDH1/2* mutations [72.7 % (8 of 11) vs. 58.3 % (7 of 12), p = 0.4672], and between AA with and without *IDH1/2* mutations [60 % (3 of 5) vs. 50 % (4 of 8), p = 0.7244]. We observed seven secondary GBMs that progressed from three DAs and four AAs without *IDH1/2* mutations, as well as eight secondary GBMs derived from five DAs and three AAs with *IDH1/2* mutations (Table 3).

Median time to malignant progression was 113.5 months and 86.4 months in DA with and without *IDH1/2* mutations, respectively ($p = 0.8360$). Median time to malignant progression was 45.3 and 19.2 months in AA with and without *IDH1/2* mutations, respectively ($p = 0.1681$).

Oligodendroglial tumors

IDH1/2 mutations were observed in 12 of 17 (70.6 %) oligodendroglial tumors. Malignant progression was observed in 47.1 % (8 of 17) oligodendroglial tumors; 33.3 % (4 of 12) were oligodendroglial tumors with *IDH1/2* mutations, and 80 % (4 of 5) were those with wild-type *IDH1/2*. Of eight patients with *IDH1/2* mutated OL/OA, four (50 %) remained OL/OA, and four (50 %) developed to AO/AOA (2 AOA and 2 AO). One patient (100 %) with wild-type *IDH1/2* OA progressed to AOA. All four patients with *IDH1/2* mutated AO/AOA were diagnosed with either AOA or AO at recurrence. One patient with *IDH1/2* mutated AO underwent tumor resection five times, and all the histopathology showed oligodendroglial components at each surgery, resulting in a diagnosis of AO (Fig. 1). Of four patients with wild-type *IDH1/2* AO/AOA, one (25 %) was diagnosed with AO at recurrence, and three were diagnosed with GBM at recurrence as determined 9.8, 14.2, and 29.1 months after the initial operation (Fig. 2; Table 3).

All 12 patients with *IDH1/2* mutated oligodendroglial tumors were diagnosed with oligodendroglial tumors at recurrence, whereas three of five patients with wild-type *IDH1/2* oligodendroglial tumors were diagnosed with GBM at recurrence. No tumors with *IDH1/2* mutated OL/OA or AO/AOA progressed to GBM. There was no particular difference in either the clinical presentation or therapeutic approach among five patients with wild-type *IDH1/2* oligodendroglial tumors. All five of these patients

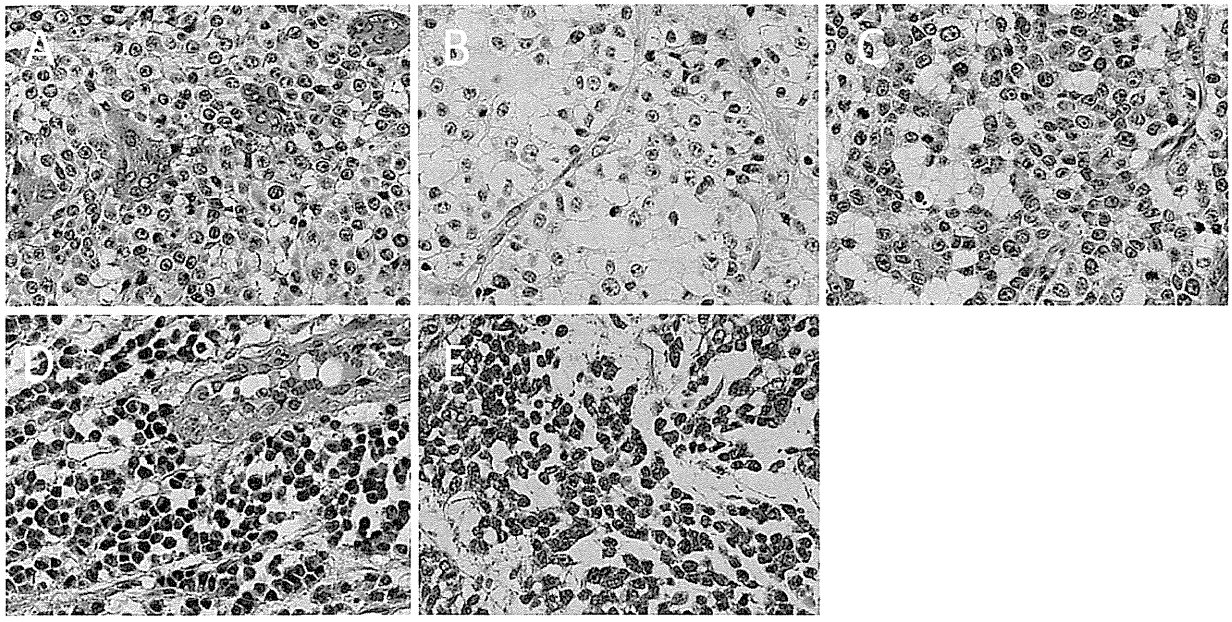

Fig. 1 Case AO 027: A-39-year-old man was diagnosed with AO at the initial operation [**a**: hematoxylin and eosin (H&E) stain, × 400]. He underwent tumor resection five times. He was diagnosed with AO at the second operation (**b**: H&E stain, ×400), AO at the third operation (**c**: H&E stain, ×400), AO at the fourth operation (**d**: H&E stain, ×400), and AO at the fifth operation (**e**: H&E stain, ×400). The tumor had the IDH1 mutation, as confirmed by direct sequence

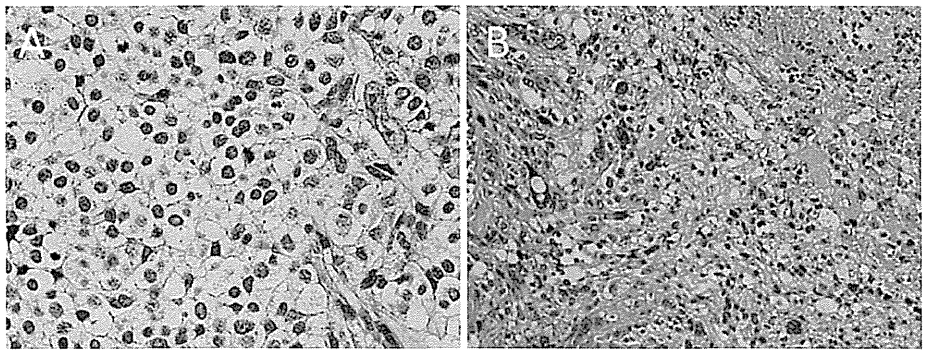

Fig. 2 Case AOA 025: A 47-year-old female was diagnosed with AOA at the initial biopsy. She was diagnosed with AOA at the second operation 24 months after the initial operation (**a**: H&E stain, ×400) and with GBM at the third operation 5 months after the second operation (**b**: H&E stain, ×200). The tumor had wild-type IDH1 and 2, as confirmed by direct sequence

received radiotherapy at the initial diagnosis, and four of them received chemotherapy (Table 3).

The frequency of malignant progression did not differ between OL/OA with and without *IDH1/2* mutations [50 % (4 of 8) vs. 100 % (1 of 1), $p = 0.2588$], whereas it was significantly higher in AO/AOA without *IDH1/2* mutations (75 %, 3 of 4) than in AO/AOA with *IDH1/2* mutations (0 %, 0 of 4, $p = 0.0136$). Median time to malignant progression was 123.8 and 4.7 months in OL/OA with and without *IDH1/2* mutations, respectively ($p = 0.0047$). Median time to malignant progression was 75.2 and 21.7 months in AO/AOA with and without *IDH1/2* mutations, respectively ($p = 0.2505$).

Discussion

We performed a longitudinal study of the histopathological alterations of grade II and III gliomas after tumor recurrence and analyzed the impact of *IDH1/2* mutations on malignant progression. Our results showed that grade II and III astrocytic tumors progressed to more malignant

histological types and eventually to GBM irrespective of the *IDH1/2* mutation status. Grade II oligodendroglial tumors with and without *IDH1/2* mutations also progressed to more malignant histological types. However, oligodendroglial tumors with *IDH1/2* mutations maintained their oligodendroglial phenotype at tumor recurrence and never progressed to GBM, whereas a fraction of grade III oligodendroglial tumors without the *IDH1/2* mutation were diagnosed with GBM at recurrence and showed a short clinical course.

The incidence of malignant progression in grade II and III gliomas is reported to be 50–90 % [14–20]. In the present study, malignant progression was observed in 68.8 % (11 of 16) and 55 % (11 of 20) of astrocytic tumors with and without *IDH1/2* mutations, and in 36.3 % (4 of 11) and 80 % (4 of 5) of oligodendroglial tumors with and without *IDH1/2* mutations, respectively. We also observed secondary GBM progressed from lower grade astrocytic tumors either with or without *IDH1/2* mutations. These observations suggest that grade II and III astrocytomas have an intrinsic potential for malignant progression, irrespective of the *IDH1/2* status. Secondary GBM also developed from grade III oligodendroglial tumors without *IDH1/2* mutations, however, not from oligodendroglial tumors with *IDH1/2* mutations. The rate of malignant progression of oligodendroglial tumors with the *IDH1/2* mutations was 33.3 %, which was relatively low compared to that of astrocytic tumors. This may indicate the indolent nature of oligodendroglial tumors with *IDH1/2* mutations [14, 15].

We found no clear correlation between the time to malignant progression and *IDH1/2* status, although it tended to be longer in *IDH1/2* mutated tumors than in *IDH1/2* wild-type tumors. Tumor recurrence or malignant progression has been shown to be associated with preoperative contrast enhancement [17, 21], tumor size [22], extent of resection [14, 22, 23], and astrocytoma pathology [14]. Considering the prior reports demonstrating that grade II and III gliomas with *IDH1/2* mutations are associated with better prognosis [9, 24], the time to malignant progression might be expected to differ depending on the *IDH1/2* status. A larger scale study in the future may provide a clearer answer as to this issue.

The diagnosis of oligodendroglial tumors is based solely on morphology, which inevitably tends to be subjective. To make histopathological diagnosis of grade III oligodendroglial tumors is particularly difficult, and diagnoses frequently differ between pathologists because some of them do not show classic oligodendroglial features [25]. We found that the *IDH1/2* status was closely related to alterations in the tumor phenotype at the recurrence. All 12 oligodendroglial tumors with *IDH1/2* mutations maintained their oligodendroglial phenotype at progression, whereas three of five tumors without *IDH1/2* mutations were diagnosed with GBM at recurrence.

With regard to the molecular aspect, Lavon et al. reported that 80 % of oligodendroglial tumors with 1p deletion maintained the oligodendroglial phenotype at progression regardless of tumor grade, whereas 62.5 % of oligodendroglial tumors with an intact 1p showed a change of phenotype to a predominantly astrocytic neoplasm at progression. The authors concluded that oligodendroglial tumors with 1p/19q deletions tended to retain their cell lineage, while tumors with intact 1p often progressed to a predominant astrocytic lineage [16]. Furthermore, *IDH1/2* mutations are strongly correlated with complete 1p/19q codeletion [26], which is associated with the classical oligodendroglial phenotype [27]. Our observations and the findings of published reports suggest that oligodendroglial tumors harboring both *IDH1/2* mutations and 1p/19q codeletion are genetically "true" oligodendroglial tumors and recur as oligodendroglial tumors without developing to GBM. Oligodendroglial tumors without *IDH1/2* mutations are heterogeneous and can therefore recur as oligodendroglial tumors or progress to GBM. Although monitoring of the *IDH1/2* status is not sufficient to differentiate oligodendroglial tumors without *IDH1/2* mutations from primary GBM, this genetic information might be a useful molecular marker to predict whether oligodendroglial tumors will develop to GBM or not at the time of tumor recurrence. Evaluation of 1p/19q codeletion status may also provide additional information. Therefore, oligodendroglial tumors without *IDH1/2* mutations should be treated intensively with careful observation.

This study has some limitations. Possible sampling errors and inter-observer variability may have affected the results because this study relied on routine histopathological diagnosis. The longitudinal histopathological alterations observed in this study were the result of the intervening chemotherapy and/or radiotherapy, and were not dependent on the intrinsic nature of the tumor. In addition, the *IDH1/2* status could not be assessed by direct sequence in all cases because of unavailability or unsuitability for direct sequencing in some specimens. Because the frequencies of IDH1 mutations other than the R132H and IDH2 mutations in grade II and III gliomas are reported to be 7.0 and 4.2 % [6, 12], we cannot completely exclude the possibility that some IHC-negative tumors may contain IDH mutations other than the R132H IDH1 mutation. Furthermore, the number of patients included in the study was small and may not be sufficient to draw a firm conclusion, especially for oligodendroglial tumors.

In conclusion, we evaluated the histological alterations of grade II and III gliomas after tumor recurrences in correlation with the *IDH1/2* status. Grade II and III astrocytomas showed the potential to progress to more

malignant histological types, irrespective of the *IDH1/2* mutation status. Oligodendroglial tumors with *IDH1/2* mutations maintained their oligodendroglial phenotype at tumor recurrence and did not progress to GBM, whereas those without *IDH1/2* mutations had the potential to progress to GBM at recurrence. Monitoring of the *IDH1/2* status could be useful to predict the development of GBM in patients with oligodendroglial tumors.

Acknowledgments This work was supported in part by the National Cancer Center Research and Development Fund (H22-55).

References

1. Louis DN, Ohgaki H, Wiestler OD, Cavenee WK (2007) WHO classification of tumours of the central nervous system, 4th edn. International Agency for Research on Cancer (IARC), Lyon
2. Jeuken JW, Sprenger SH, Vermeer H et al (2002) Chromosomal imbalances in primary oligodendroglial tumors and their recurrences: clues about malignant progression detected using comparative genomic hybridization. J Neurosurg 96:559–564
3. Ohgaki H, Kleihues P (2011) Genetic profile of astrocytic and oligodendroglial gliomas. Brain Tumor Pathol 28:177–183
4. Miller CR, Dunham CP, Scheithauer BW, Perry A (2006) Significance of necrosis in grading of oligodendroglial neoplasms: a clinicopathologic and genetic study of newly diagnosed high-grade gliomas. J Clin Oncol 24:5419–5426
5. Balss J, Meyer J, Mueller W et al (2008) Analysis of the IDH1 codon 132 mutation in brain tumors. Acta Neuropathol 116:597–602
6. Hartmann C, Meyer J, Balss J et al (2009) Type and frequency of IDH1 and IDH2 mutations are related to astrocytic and oligodendroglial differentiation and age: a study of 1,010 diffuse gliomas. Acta Neuropathol 118:469–474
7. Ichimura K, Pearson DM, Kocialkowski S et al (2009) IDH1 mutations are present in the majority of common adult gliomas but rare in primary glioblastomas. Neuro Oncol 11:341–347
8. Watanabe T, Nobusawa S, Kleihues P, Ohgaki H (2009) IDH1 mutations are early events in the development of astrocytomas and oligodendrogliomas. Am J Pathol 174:1149–1153
9. Yan H, Parsons DW, Jin G et al (2009) IDH1 and IDH2 mutations in gliomas. N Engl J Med 360:765–773
10. Kim YH, Nobusawa S, Mittelbronn M et al (2010) Molecular classification of low-grade diffuse gliomas. Am J Pathol 177:2708–2714
11. Ichimura K. (2012) Molecular pathogenesis of IDH mutations in gliomas. Brain Tumor Pathol
12. Reitman ZJ, Yan H (2010) Isocitrate dehydrogenase 1 and 2 mutations in cancer: alterations at a crossroads of cellular metabolism. J Natl Cancer Inst 102:932–941
13. Capper D, Reuss D, Schittenhelm J et al (2011) Mutation-specific IDH1 antibody differentiates oligodendrogliomas and oligoastrocytomas from other brain tumors with oligodendroglioma-like morphology. Acta Neuropathol 121:241–252
14. Chaichana KL, McGirt MJ, Laterra J et al (2010) Recurrence and malignant degeneration after resection of adult hemispheric low-grade gliomas. J Neurosurg 112:10–17
15. Jaeckle KA, Decker PA, Ballman KV et al (2010) Transformation of low grade glioma and correlation with outcome: an NCCTG database analysis. J Neurooncol 104:253–259
16. Lavon I, Zrihan D, Zelikovitch B et al (2007) Longitudinal assessment of genetic and epigenetic markers in oligodendrogliomas. Clin Cancer Res 13:1429–1437
17. McCormack BM, Miller DC, Budzilovich GN et al (1992) Treatment and survival of low-grade astrocytoma in adults—1977–1988. Neurosurgery 31:636–642 discussion 642
18. Ohgaki H, Kleihues P (2005) Population-based studies on incidence, survival rates, and genetic alterations in astrocytic and oligodendroglial gliomas. J Neuropathol Exp Neurol 64:479–489
19. Schmidt MH, Berger MS, Lamborn KR et al (2003) Repeated operations for infiltrative low-grade gliomas without intervening therapy. J Neurosurg 98:1165–1169
20. van den Bent MJ, Afra D, de Witte O et al (2005) Long-term efficacy of early versus delayed radiotherapy for low-grade astrocytoma and oligodendroglioma in adults: the EORTC 22845 randomised trial. Lancet 366:985–990
21. Kreth FW, Faist M, Rossner R et al (1997) Supratentorial World Health Organization Grade 2 astrocytomas and oligoastrocytomas. A new pattern of prognostic factors. Cancer 79:370–379
22. Berger MS, Deliganis AV, Dobbins J, Keles GE (1994) The effect of extent of resection on recurrence in patients with low grade cerebral hemisphere gliomas. Cancer 74:1784–1791
23. Claus EB, Horlacher A, Hsu L et al (2005) Survival rates in patients with low-grade glioma after intraoperative magnetic resonance image guidance. Cancer 103:1227–1233
24. Sanson M, Marie Y, Paris S et al (2009) Isocitrate dehydrogenase 1 codon 132 mutation is an important prognostic biomarker in gliomas. J Clin Oncol 27:4150–4154
25. Coons SW, Johnson PC, Scheithauer BW et al (1997) Improving diagnostic accuracy and interobserver concordance in the classification and grading of primary gliomas. Cancer 79:1381–1393
26. Labussiere M, Idbaih A, Wang XW et al (2010) All the 1p19q codeleted gliomas are mutated on IDH1 or IDH2. Neurology 74:1886–1890
27. Giannini C, Burger PC, Berkey BA et al (2008) Anaplastic oligodendroglial tumors: refining the correlation among histopathology, 1p 19q deletion and clinical outcome in Intergroup Radiation Therapy Oncology Group Trial 9402. Brain Pathol 18:360–369

Cancer Science
The official journal of the Japanese Cancer Association JCA

Importance of direct macrophage - Tumor cell interaction on progression of human glioma

Yoshihiro Komohara,[1,5] Hasita Horlad,[1,5] Koji Ohnishi,[1] Yukio Fujiwara,[1] Bing Bai,[1] Takenobu Nakagawa,[1] Shinya Suzu,[2] Hideo Nakamura,[3] Jun-ichi Kuratsu[3] and Motohiro Takeya[1,4]

[1]Department of Cell Pathology, Graduate School of Medical Sciences, Kumamoto University, Kumamoto; [2]Center for AIDS Research, Kumamoto University, Kumamoto; [3]Department of Neurosurgery, Graduate School of Medical Sciences, Kumamoto University, Kumamoto, Japan

(Received July 10, 2012/Revised August 31, 2012/Accepted September 2, 2012/Accepted manuscript online September 7, 2012/Article first published online October 26, 2012)

We previously showed tumor-associated macrophages/microglia (TAMs) polarized to the M2 phenotype were significantly involved in tumor cell proliferation and poor clinical prognosis in patients with high grade gliomas. However, the detailed molecular mechanisms involved in the interaction between TAMs and tumor cells have been unclear. Current results reveal that, in coculture with human macrophages, BrdU incorporation was significantly elevated in glioma cells, and signal transducer and activator of transcription-3 (Stat3) activation was found in both cell types. Direct mixed coculture led to stronger Stat3 activation in tumor cells than did indirect separate coculture in Transwell chamber dishes. Screening with an array kit for phospho-receptor tyrosine kinases revealed that phosphorylation of macrophage-colony stimulating factor receptor (M-CSFR, CD115, or *c-fms*) is possibly involved in this cell–cell interaction; M-CSFR activation was detected in both cell types. Coculture-induced tumor cell activation was suppressed by siRNA-mediated downregulation of the M-CSFR in macrophages and by an inhibitor of M-CSFR (GW2580). Immunohistochemical analysis of phosphorylated (p) M-CSFR, pStat3, M-CSF, M2 ratio, and MIB-1(%) in high grade gliomas revealed that higher staining of pM-CSFR in tumor cells was significantly associated with higher M-CSF expression and higher MIB-1(%). Higher staining of pStat3 was associated with higher MIB-1(%). High M2 ratios were closely correlated with high MIB-1(%) and poor clinical prognosis. Targeting these molecules or deactivating M2 macrophages might be useful therapeutic strategies for high grade glioma patients. (*Cancer Sci* 2012; 103: 2165–2172)

Macrophages that infiltrate cancer tissues are called tumor-associated macrophages (TAMs) and are closely involved in development of the tumor microenvironment by inducing angiogenesis, immunosuppression, and invasion.[1,2] Tumor-associated macrophages are generally thought to belong to the alternatively activated macrophage population (M2) because of their anti-inflammatory functions.[3] In many kinds of malignant tumors, including melanoma, malignant lymphoma, leiomyosarcoma, pancreatic tumors, intrahepatic cholangiocarcinoma, renal cell carcinoma, and high grade glioma, the presence of M2-polarized TAMs is associated with poor clinical prognosis.[4–11] Although it is well known that many TAMs infiltrate into high grade gliomas and are associated with angiogenesis and immunosuppression,[12–15] results of this study show that M2-polarized TAMs are significantly involved in glioma tumor cell proliferation and are related to poor prognosis of high grade glioma patients.[6]

Signal transducer and activator of transcription-3 (Stat3) affects the tumor microenvironment and tumor development by virtue of its association with immunosuppression, angiogenesis, and cancer cell proliferation.[16,17] In some kinds of malignant tumors, including high grade glioma, patients with high Stat3 activation in tumor cells have significantly worse clinical prognosis.[18] Therefore, Stat3 is thought to be an important target molecule for anticancer therapy, and many researchers have introduced various kinds of Stat3 inhibitors as anticancer drugs.[19] Stat3 signaling in macrophages is known to participate in regulating immune responses. Targeted disruption of Stat3 signaling resulted in activation of antigen-specific T cells, and suppressed tumor development in murine cancer models.[20–22] In patients with glioblastoma, inhibition of Stat3 not only suppressed tumor cell growth but also reversed immune tolerance by impairing the immune-suppressive function of alternatively activated macrophage/microglia.[23]

In this study, M2 macrophages were found to support proliferation of glioma cells through Stat3 activation. Cell–cell interaction during direct contact between tumor cells and macrophages contributes to strong activation of macrophages, which in turn activates tumor cells. *In vitro* results of the use of a receptor-type tyrosine kinase (RTK) array revealed the importance of macrophage-colony stimulating factor receptor (M-CSFR) activation in this cell–cell interaction. The crucial role of macrophage-colony stimulating factor (M-CSF), especially membrane-type M-CSF (mM-CSF), and its binding to M-CSFR during direct cell–cell interactions between tumor cells and macrophages was determined.

Materials and Methods

Macrophage culture. Peripheral blood mononuclear cells were obtained from three healthy volunteer donors and written informed consent for experimental use of the same was supplied by all donors. $CD14^+$ monocytes were isolated using CD14 microbeads (Miltenyi Biotec, Bergisch Gladbach, Germany). Monocytes were plated in 6-well (1×10^5/well) or 12-well (5×10^4/well) plates and cultured with granulocyte M-CSF (2 ng/mL) (Wako, Tokyo, Japan) for 5 days to induce immature macrophages. After PBS washes, cells were stimulated with γ-interferon (1 ng/mL) (PeproTech, Rocky Hill, NJ, USA) to induce M1 macrophages. These cells were stimulated with 50% tumor-cell supernatant (TCS) to induce M2 macrophages, because TCS contains many anti-inflammatory cytokines and pushes macrophage polarization toward the M2 phenotype.[6]

Cell lines. Tumor-cell supernatant was prepared as described previously.[6] The human glioblastoma cell line T98G was purchased from ATCC (Manassas, VA, USA) and was maintained in DMEM supplemented with 10% FBS, 100 U/mL penicillin, 100 μg/mL streptomycin, and 0.1 mg/mL sodium pyruvate. The mycoplasma test was carried out using a PCR detection kit (Takara Bio, Otsu, Japan). Human myeloid leukemia TF-1

[4]To whom correspondence should be addresssed.
E-mail: takeya@kumamoto-u.ac.jp
[5]These authors contributed equally to this work.

doi: 10.1111/cas.12015

cells expressing M-CSFR were cultured in DMEM with 10% FBS and granulocyte M-CSF, as described previously.[24]

Coculture experiment. To investigate the cell–cell interaction between tumor cells and macrophages, coculture experiments were carried out as described previously.[25] Briefly, after macrophages were washed in PBS, they were co-incubated with T98G cells for 2 days to evaluate the significance of direct cell–cell contact. To examine the influence of indirect cell–cell

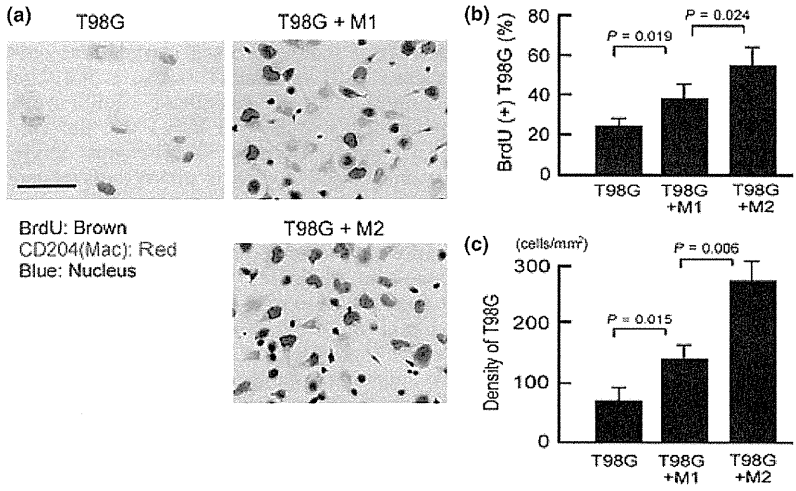

Fig. 1. Tumor cell proliferation by coculture with macrophages. (a) Primary monocyte-derived macrophages were stimulated with γ-interferon (M1) or tumor-cell supernatant (M2), and cocultured with T98G cells for 2 days. Double immunostaining of CD204 and BrdU was carried out to evaluate BrdU incorporation by tumor cells. $CD204^+$ cells (red) indicate macrophages. (b) $BrdU^+$ cells among $CD204^-$ tumor cells were counted under a microscope. (c) The number of tumor cells per 1 mm^2 was counted under a microscope.

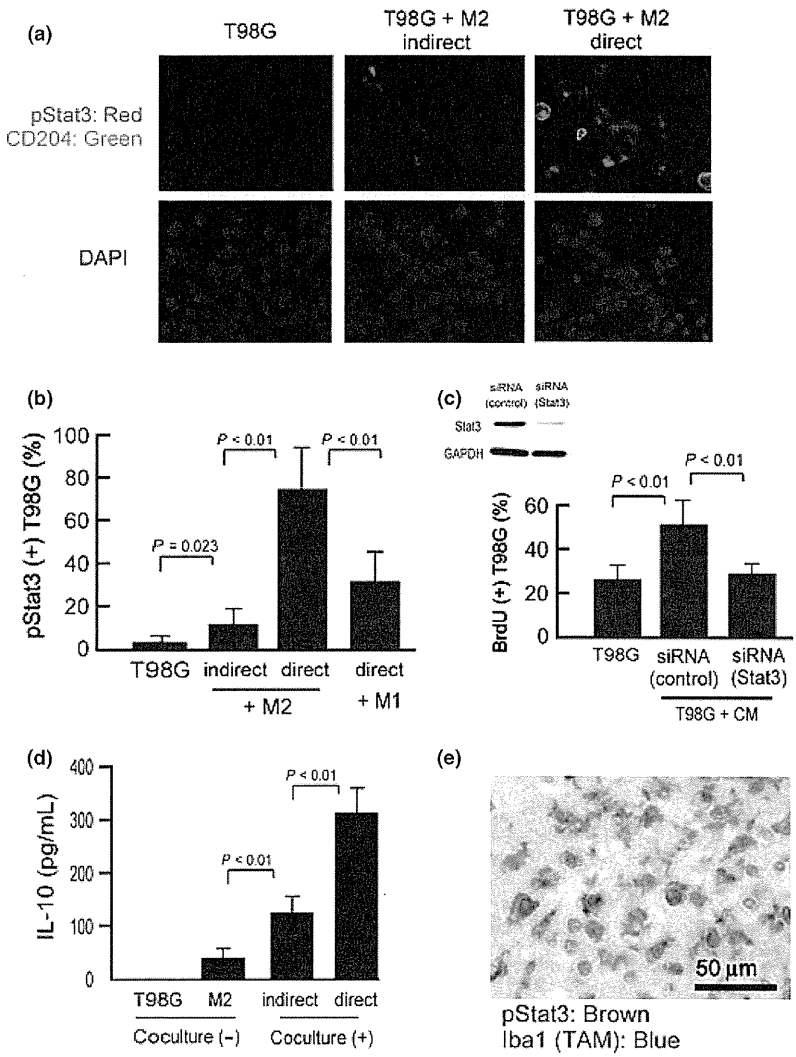

Fig. 2. Signal transducer and activator of transcription-3 (Stat3) activation in cocultured cells. (a) T98G cells were cocultured with tumor-cell supernatant-stimulated M2 macrophages, and Stat3 activation was analyzed by double immunostaining of pStat3 (red) and CD204 (green). Blue indicates nuclear staining. Scale bar = 50 μm. (b) Following double immunostaining, 100 $CD204^-$ T98G cells were counted, and the percentage of $pStat3^+$ cells was calculated (n = 3 or 4 for each group). (c) BrdU incorporation in conditional medium-stimulated T98G cells was evaluated with or without Stat3 siRNA. (n = 3 for each group). Downregulation of Stat3 protein in T98G cells was also confirmed by Western blot analysis. (d) Interleukin (IL)-10 production was evaluated as a marker of macrophage activation (n = 4 for each group). (e) Double immunostaining of activated Stat3 (brown) and Iba-1 (marker of macrophages/microglia; blue) was carried out.

doi: 10.1111/cas.12015

interaction, Transwell chamber dishes (Nunc, Rochester, NY, USA) were used.

BrdU incorporation and immunostaining. BrdU incorporation and immunostaining was carried out using the BrdU ELISA kit (Roche, Basel, Switzerland) according to the manufacturer's protocol with minor modifications. Briefly, after culture with BrdU for 90 min, cells were fixed by acetone. CD204 (clone SRA-E5; Transgenic, Kumamoto, Japan) was stained and visualized using the Warp Red chromogen kit (Biocare Medical, Concord, CA, USA). After washes in glycine buffer (pH 2.2), cells were stained with anti-BrdU antibody and visualized using the diaminobenzidine substrate system (Nichirei, Tokyo, Japan).

Immunofluorescence staining of pStat3. Paraffin-embedded cell block specimens were prepared and sectioned as described previously.[25] Mounted sections were deparaffinized in xylene and rehydrated in a graded ethanol series. Following treatment for antigen retrieval, sections were reacted with anti-CD204 antibody (mouse monoclonal, clone SRA-E5) and anti-pStat3 antibody (Tyr705, clone D3A7; Cell Signaling Technology, Denver, MA, USA). Antibodies were diluted with CanGetSignal (Toyobo, Tokyo, Japan). Alexa Fluor 488 goat anti-mouse IgG and Alexa Fluor 546 goat anti-rabbit IgG (Invitrogen, Camarillo, CA, USA) were used as secondary antibodies.

Inhibitor. The M-CSFR inhibitor GW2580 (Calbiochem, Nottingham, UK) was used at either 20 nM or 30 nM concentrations.

Small interfering RNA in human macrophages. Human macrophages were transfected with siRNA against human Stat3 (Santa Cruz Biotechnology, Santa Cruz, CA, USA) or M-CSFR (Santa Cruz Biotechnology) using Lipofectamine RNAi MAX (Invitrogen). Control siRNA (Santa Cruz Biotechnology) was used as a negative control. Downregulation of Stat3 and M-CSFR was evaluated by Western blot and real-time PCR, respectively, as described previously.[9]

Evaluation of cytokine secretion in supernatant. The interleukin (IL)-10 concentration in supernatants was determined using ELISA kits (PeproTech).

Phospho-receptor tyrosine kinase array analysis. The relevant phospho-receptor tyrosine kinase (RTK) array was purchased from R&D Systems (Minneapolis, MN, USA), and used according to the manufacturer's protocol.

Flow cytometry. Cells were detached from wells using enzyme-free Cell Dissociation Buffer (Gibco, Grand Island, NY, USA) and immediately fixed with 4% paraformaldehyde. After incubation with 0.1% saponin, cells were reacted with anti-pM-CSFR antibody and anti-CD68 antibody (mouse monoclonal, clone PM-1K[26]). Then FITC-labeled anti-mouse IgG and phycoerythrin-labeled anti-rabbit IgG were used as secondary antibodies, and cells were analyzed by FACSCalibur.

Human glioblastoma samples. From January 2006 to September 2009, paraffin-embedded tissue samples from 62 patients with high grade gliomas (nine patients with anaplastic astrocytoma and 53 patients with glioblastoma) were prepared for this study. Cases with massive necrosis were not enrolled. Informed written consent was obtained from all patients in accordance with protocols approved by the Kumamoto University Review Board. Tissue samples were fixed in 10% neutral buffered formalin and were embedded in paraffin.[6]

Immunostaining and double immunostaining of surgical specimens. Sections were deparaffinized in xylene and rehydrated in a graded ethanol series. Anti-pStat3 antibody (clone D3A7; Cell Signaling Technology), anti-pM-CSFR antibody (Tyr 723, clone 49C10; Cell Signaling Technology), anti-M-CSF antibody (clone EP1179Y; Novus Biologicals, Littleton, CO, USA), anti-CD163 antibody (clone 10D6; Novocastra, Newcastle, UK), anti-Iba-1 (polyclonal; Wako), and anti-Ki-67 (clone MIB-1; Dako, Glostrup, Denmark) were used as primary antibodies. Horseradish peroxidase-labeled or alkaline phosphatase-labeled antibodies (Nichirei) were used as secondary antibodies. Reactions were visualized by the diaminobenzidine system (Nichirei), Fast Blue solution (Sigma, St. Louis, MO, USA), or HistoGreen (Linaris Biologische, Wertheim-Bettingen, Germany). Macrophage-colony stimulating factor receptor activation and M-CSF expression was scored as 0 (negative), 1 (weak), or 2 (strong) by two pathologists (Y.K. and H.H.) who were blind to the sample data, then the sum of scores for each sample was categorized as "low" (score 0–2) or "high" (score 3–4). The MIB-1 index and M2 ratio ($CD163^+$ cells/$Iba\text{-}1^+$ cells) were determined by two pathologists (Y.K. and H.H.) and the values obtained were averaged. Because a previous study showed that the ratio of $CD163^+$ TAMs is closely correlated with tumor cell proliferation and clinical prognosis,[6] patients were divided into two M2 ratio groups, low (<30%) and high ($\geq$30%). Stat3 activation was scored as 0 to 8 as described previously,[27] then the sum of scores for each sample was categorized as "low" (score 0–4) or "high" (score 5–8).

Statistics. Statistical analysis of *in vitro* and *in vivo* data was carried out using JMP10 (SAS Institute, Chicago, IL, USA). All data from *in vitro* studies represent results of two or three independent experiments. Data are expressed as the mean ± SD. The Mann–Whitney *U*-test was used for two-group comparisons. A value of $P < 0.05$ was considered statistically significant.

Results

Glioblastoma cells were activated by coculture with M2 macrophages. In the first experiments, the effects of cell–cell interaction between macrophages and T98G cells were investigated by means of the coculture system. BrdU incorporation into T98G cells was evaluated by double immunostaining, and was found to be significantly upregulated by coculture with macrophages; M2, rather than M1, cells caused a notable increase of BrdU incorporation by T98G cells (Fig. 1a,b).

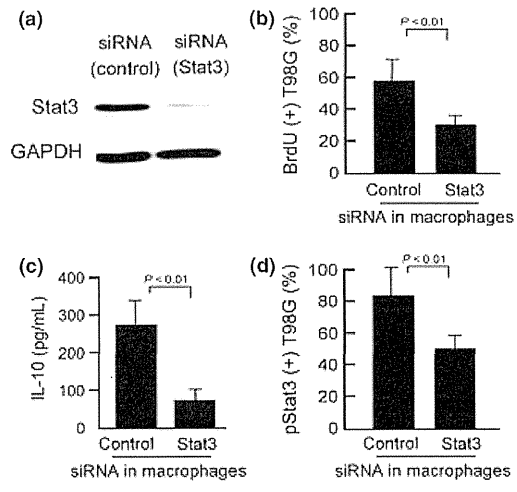

Fig. 3. Effect of selective signal transducer and activator of transcription-3 (Stat3) silencing in macrophages on Stat3 activation in glioma cells. (a) Western blot analysis confirmed suppression of Stat3 in macrophages. (b) Two days after suppression of Stat3 in macrophages, T98G cells were added to the culture. After coculture for 2 days, double immunostaining of CD204 and BrdU was carried out. Percentages of $BrdU^+$ cells among $CD204^-$ tumor cells were calculated. (c) In the same conditions, interleukin (IL)-10 concentration in supernatants was determined. (d) After the same treatment, cells were prepared as cell block specimens and double immunostaining of CD204 and pStat3 was done. Percentages of $pStat3^+$ cells among the $CD204^-$ tumor cells were calculated.

The proliferation of T98G cells was increased by coculture with M1 and M2, but notably higher proliferation was induced by M2 (Fig. 1c).

As Stat3 is one of the signaling molecules related to cell proliferation and survival, Stat3 activation was evaluated in the coculture system. When M2 cells and T98G cells were cocultured, both cell types showed strong nuclear staining of pStat3 (Fig. 2a,b). In contrast to indirect coculture conditions, direct cell–cell interaction caused significantly stronger Stat3 activation in cancer cells (Fig. 2b). Stat3 activation in T98G cells was more strongly induced by coculture with M2 cells compared with M1 cells (Fig. 2b). The proliferation of T98G cells was induced by stimulation with conditional medium of cocultured M2 cells and T98G cells, and this effect was significantly suppressed by blocking Stat3 in T98G cells (Fig. 2c).

To evaluate macrophage activation in the coculture system, IL-10 concentrations in supernatants were determined, because no IL-10 secretion was detected in supernatants of T98G cell monocultures. As shown in Figure 2(d), IL-10 secretion was induced by coculture and, notably, direct coculture induced significantly increased IL-10 secretion. We next evaluated Stat3 activation in human glioma tissues. Among 12 high grade glioma samples analyzed, 10 showed distinct infiltration of $pStat3^{+}$ TAMs (Fig. 2e). These observations indicate a critical role for Stat3 in cell–cell interaction between tumor cells and macrophages.

Activation of Stat3 involved in cell–cell interaction between glioma cells and macrophages. We next suppressed Stat3 in M2 macrophages using siRNA before coculture with T98G cells to ascertain whether Stat3 activation in macrophages contributes

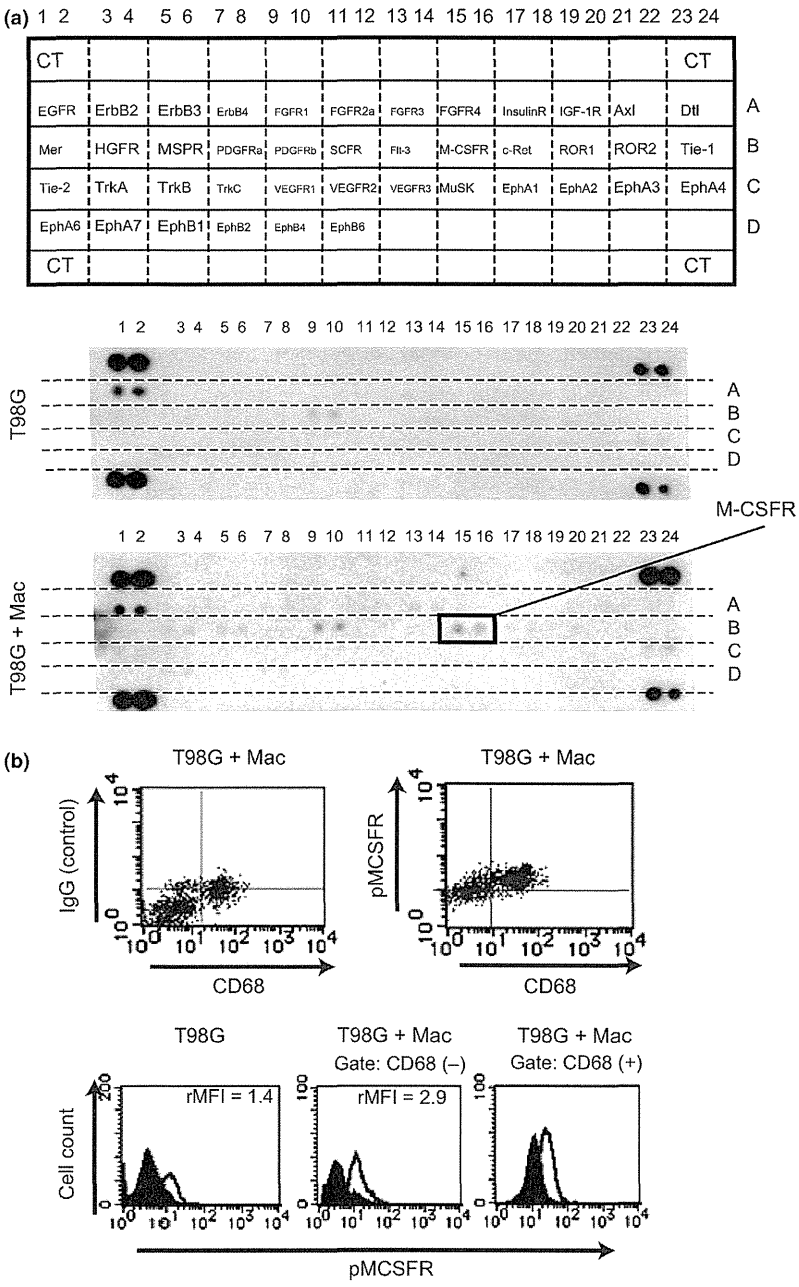

Fig. 4. Receptor-type tyrosine kinase array and flow cytometry. (a) Receptor-type tyrosine kinase array analyses were carried out and results for cocultured cells (T98G + Mac) and T98G cells in monoculture (T98G) were compared. CT, positive control. (b) Phosphorylation of macrophage colony-stimulating factor receptor (M-CSFR) was evaluated by flow cytometry. Representative data from one of two experiments.

doi: 10.1111/cas.12015

to the cell–cell interaction (Fig. 3a,b). Incorporation of BrdU into T98G cells was significantly inhibited by Stat3 suppression in macrophages (Fig. 3b). Secretion of IL-10 from macrophages was also inhibited by Stat3 suppression (Fig. 3c). As Figure 3(d) shows, Stat3 activation in T98G cells was decreased by blocking Stat3 in macrophages. These data indicate that macrophage activation through Stat3 signaling is important for tumor cell activation in coculture.

Activation of M-CSFR involved in cell–cell interaction. Direct contact with tumor cells significantly induced macrophage activation. Therefore, we hypothesized that RTK mediates this effect, and RTK array analysis was carried out. Activation of RTK in cocultured cells was compared with that of macrophages and T98G cells cultured separately, and significant activation of M-CSFR was found in cocultured macrophages (Fig. 4a), as well as, interestingly, in the cocultured T98G cells (Fig. 4b).

Activation of M-CSFR involved in macrophage activation by direct cell–cell interaction, and induced Stat3 activation in tumor cells. Next, we investigated whether M-CSFR is involved in

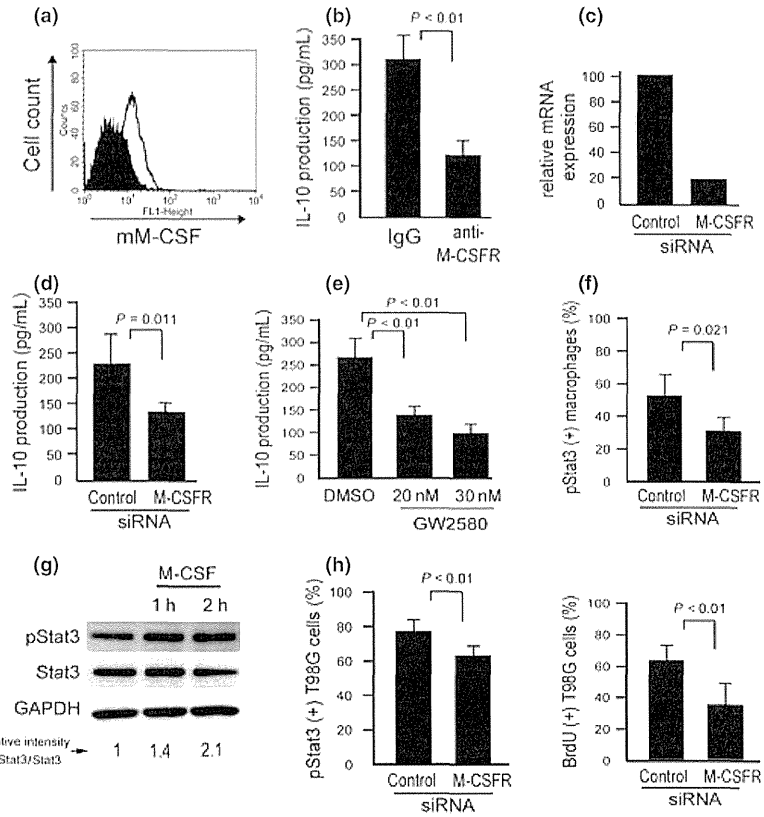

Fig. 5. Involvement of macrophage colony-stimulating factor receptor (M-CSFR) in direct cell–cell interaction. (a) Membrane-type M-CSF (mM-CSF) was expressed on the surface membranes of T98G cells. (b) T98G cells were cocultured with macrophages in the presence of anti-M-CSF antibody for 2 days, and interleukin (IL)-10 in the supernatant was measured by ELISA. Non-immunized rabbit IgG was used as the control. (c) Downregulation of M-CSFR by siRNA was confirmed by real-time PCR. (d) T98G cells were cocultured with macrophages having silenced M-CSFR for 2 days, and IL-10 in the supernatant was measured. (e) Macrophages and T98G cells were mixed and cultured with the M-CSFR inhibitor GW2580 for 2 days, and IL-10 in the supernatant was measured. (f) M-CSFR of macrophages was silenced by siRNA, and coculture proceeded for 2 days. Signal transducer and activator of transcription-3 (Stat3) activation in macrophages was evaluated by double immunostaining. (g) Macrophages were stimulated with M-CSF (100 ng/mL) for 1 or 2 h, and Stat3 activation was evaluated. (h) M-CSFR of macrophages was silenced by siRNA, and coculture proceeded. BrdU incorporation and Stat3 activation in T98G cells was examined by double immunostaining (n = 3 or 4 for each group).

Table 1. Clinicopathologic factors, macrophage-colony stimulating factor receptor (M-CSFR) activation, macrophage-colony stimulating factor (M-CSF) expression, and signal transducer and activator of transcription-3 (Stat3) activation in high grade glioma

Variable	n	M-CSFR activation		P-value	M-CSF expression		P-value	Stat3 activation		P-value
		Low	High		Low	High		Low	High	
Age, years										
<60	26	15	11	P = 0.700	12	14	P = 0.760	11	15	**P = 0.025**
≥60	36	19	17		18	18		6	30	
Gender										
Male	40	18	22	**P = 0.036**	18	22	P = 0.470	8	32	P = 0.077
Female	22	16	6		12	10		9	13	
M-CSFR activation										
Low	33	–	–	–	25	8	**P < 0.001**	11	22	P = 0.270
High	29	–	–		3	26		6	23	
M-CSF expression										
Low	30	–	–	–	–	–	–	10	20	P = 0.310
High	32	–	–		–	–		7	25	
M2 macrophages										
Low	25	15	10	P = 0.27	17	8	**P = 0.011**	9	16	P = 0.210
High	37	17	20		13	24		8	29	

Bold text indicates statistically significant results, calculated using the chi-squared test.

Table 2. Univariate Cox regression analysis of potential prognostic factors

		Univariate analysis		
	n	Mean survial (weeks)	*P*-value Log–rank	*P*-value Wilcoxon
Age, years				
<60	26	88	**0.034**	**0.006**
≥60	36	57		
Gender				
Male	40	72	0.42	0.91
Female	22	65		
pM-CSFR				
Low	34	78	0.054	0.089
High	28	64		
M-CSF				
Low	33	72	0.49	0.57
High	29	65		
Stat3 activation				
Low	17	124	0.058	0.22
High	45	85		
M2 ratio				
Low	25	98	**0.003**	**0.004**
High	37	62		
MIB-1 (%)				
<30	26	113	**0.0005**	**0.0007**
≥30	36	56		

Bold text indicates statistically significant results. M-CSF, macrophage-colony stimulating factor; pM-CSFR, phosphorylated M-CSF receptor; MIB-1, anti-Ki-67; Stat3, transducer and activator of transcription-3.

macrophage activation by coculture with T98G cells. The T98G cells expressed mM-CSF on their cell surface membranes (Fig. 5a). Neutralizing antibody for mM-CSF and silencing of M-CSFR significantly inhibited IL-10 secretion in direct coculture (Fig. 5b–d). An inhibitor of M-CSFR (GW2580) also suppressed IL-10 secretion (Fig. 5e). Activation of Stat3 was inhibited by silencing M-CSFR in macrophages (Fig. 5f) and was significantly induced by M-CSF stimulation in macrophages (Fig. 5g). These data indicate that M-CSFR signaling contributes to Stat3 activation in cocultured macrophages.

We then tested if M-CSFR signaling in macrophages influences tumor cell activation. Both BrdU incorporation and Stat3 activation in cocultured tumor cells were decreased by silencing M-CSFR in macrophages (Fig. 5h).

M2 ratio and M-CSFR activation associated with MIB-1 index in high grade glioma. Immunostaining for pM-CSFR, M-CSF, CD163, Iba-1, and MIB-1 was carried out in 62 cases of high grade glioma. Mutual correlations of their expression and the association with clinical prognosis were statistically evaluated (Tables 1,2). The specificity of anti-pM-CSFR antibody was confirmed using M-CSFR-expressing TF-1 histiocytic cells (Fig. 6a). Both M-CSF expression and M-CSFR activation, as well as M2 phenotype, were classified into two groups, high and low, as described above (Fig. 6b). A positive pM-CSFR signal was seen in both tumor cells and macrophages (Fig. 6c). Activation of Stat3 was also classified into two groups (Fig. 6d). Higher activation of M-CSFR in tumor cells was closely associated with higher M-CSF expression and a higher MIB-1 (%) (Table 1, Fig. 6d). A higher M2 ratio ($CD163^+$ cells/$Iba\text{-}1^+$ cells), higher M-CSF expression, and higher Stat3 activation was also correlated with a higher MIB-1(%) (Fig. 6e). In addition, the patients with higher ages, M2 ratios, or MIB-1(%) had statistically significant shorter survival

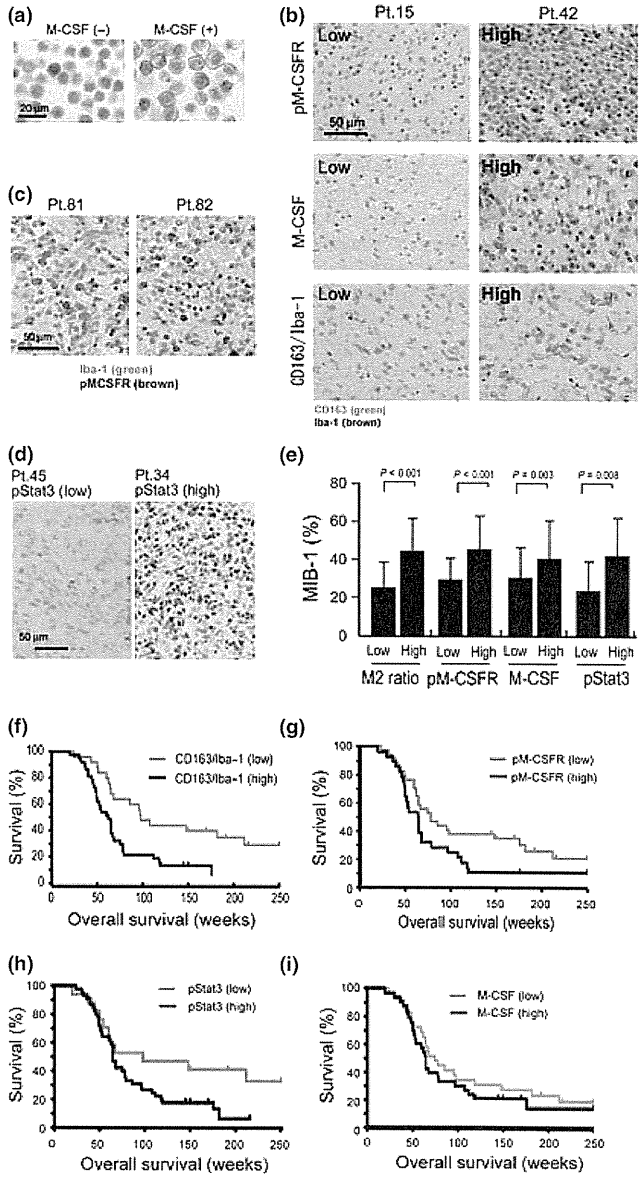

Fig. 6. Immunohistochemical determination of phosphorylated macrophage-colony stimulating factor receptor (pM-CSFR), macrophage-colony stimulating factor (M-CSF), phosphorylated signal transducer and activator of transcription-3 (pStat3), anti-Ki-67 (clone MIB-1), and M2 ratios in human high grade gliomas. (a) TF-1 culture cells were stimulated by M-CSF for 5 min and activation of M-CSFR was evaluated by immunostaining with anti-pM-CSFR. Strong activation of pM-CSFR was detected on cell surfaces of M-CSF-stimulated TF-1 cells. (b) Immunostaining of pM-CSFR, M-CSF, and double immunostaining of CD163 (green) and Iba-1 (brown) were carried out. Results for patient (Pt.) no. 15 and no. 42 are shown. (c) By double immunostaining ofIba-1 (green) and pM-CSFR (brown), pM-CSFR was detected in both tumor cells and macrophages. (d) Immunostaining of pStat3 was also carried out to evaluate the Stat3 activation in tumor cells. (e) M2 ratio, M-CSFR activation, Stat3 activation, and M-CSF expression were correlated with the MIB-1 index. The Kaplan–Meier method was used to determine (f) M2 ratio, (g) M-CSFR activation, (h) Stat3 activation and (i) M-CSF expression.

periods (Fig. 6f, Table 2). The patients with higher M-CSFR and Stat3 activation had shorter survival periods, but this result was not statistically significant (Fig. 6g,h). In

doi: 10.1111/cas.12015

addition, M-CSF expression was not significantly associated to clinical prognosis (Fig. 6i).

Discussion

The importance of TAMs in tumor growth has been well documented, and TAMs are thought to contribute to tumor progression and invasion.[28,29] In this study, we showed that direct contact with glioma cells induces macrophage activation, which in turn activates tumor cells. Macrophage activation through M-CSFR/Stat3 signaling was shown to play an important role in cell–cell interaction. Analysis of human glioma samples indicated that M-CSFR activation and M2 ratios are associated with tumor cell proliferation.

The importance of direct cell–cell contact in cell–cell interaction has been a focus for several researchers. Direct cell–cell contact between macrophages and tumor cells protected tumor cells from chemotherapy drug-induced apoptosis, whereas cell–cell interaction without direct contact did not.[30] A previous study showed that Stat3 activation in ovarian and kidney cancer cells was significantly induced by direct coculture with macrophages.[9,25] As Stat3 is associated with cancer cell proliferation and survival,[16,17] macrophages are thought to support cancer cell proliferation and survival in patients with malignant tumors. A selective Stat3 inhibitor and Stat3 siRNA reversed cytokine expression levels and suppressed tumor growth *in vivo*, and this indicated a major contribution of Stat3 signaling in the immunosuppression by glioma-derived factors.[31,32]

It is well known that mM-CSF induces stronger activation of M-CSFR than soluble M-CSF, although details of the mechanisms involved have been unclear.[33,34] In this study, the possible involvement of mM-CSF–M-CSFR binding on strong Stat3 activation in tumor microenvironment was shown. It is well known that M-CSFR signaling activates some signal molecules including Stat3 activation,[35] and the results shown in Figure 5 indicate that M-CSFR signaling was significantly related to Stat3 activation in this coculture system. Stat3 activation plays an important role in maintenance of glioma stem cells (GSCs),[36] and unknown Stat3-related cytokines derived from GSCs induce macrophage polarization into the M2 phenotype.[37] Although M-CSF expression in GSCs has, to the best of our knowledge, never been reported, the current results suggest that cell–cell interaction between macrophages and GSCs is involved in creating the stem-cell niche of high grade gliomas.

Some studies have shown the efficacy of M-CSFR inhibitors in murine cancer models. Recently, the M-CSFR inhibitor Ki20227 was shown to suppress tumor angiogenesis, lymphangiogenesis, and metastasis, and these effects were suggested to be caused by macrophage dysfunction.[38] GW2580 inhibited the recruitment of myeloid cells into tumor tissues and combination therapy with an anti-angiogenic agent significantly suppressed tumor growth.[39,40] These data indicate that blocking of M-CSFR is effective as an anticancer therapy through abrogating the functions of myeloid cells.

In a previous study, we showed that the M2 ratio of TAMs is significantly associated with high tumor cell proliferation and poor clinical prognosis in patients with high grade glioma.[6] As shown in Figure 6, the current study indicated that poor clinical prognosis was statistically significantly associated with higher M2 ratio, higher age, and higher MIB-1(%), confirming observations consistent with the previous study. In addition, M-CSFR activation in tumor cells was correlated with M-CSF expression and MIB-1(%) but not macrophage phenotype. These findings indicate that further studies are necessary to elucidate detailed mechanisms underlying the effects of cell–cell interaction in the glioma microenvironment.

Results showing that blocking M-CSFR and Stat3 in macrophages suppressed tumor cell activation indicate that some soluble factors derived from activated macrophages contribute to tumor cell activation in coculture experiments. Although we were not able to identify macrophage-derived soluble factors, it was previously reported that glioma-derived factors enhanced Stat3 activity in microglia, and induced increased production of transforming growth factor-β, IL-6, and IL10 in a murine model.[31] A selective Stat3 inhibitor and Stat3 siRNA reversed cytokine expression levels and suppressed tumor growth *in vivo*, indicating a major contribution of Stat3 signaling to immunosuppression by glioma-derived factors.[31,32]

In summary, results of the present study indicate that macrophage activation through M-CSFR/Stat3 signals plays an important role in cell–cell interaction between macrophages and tumor cells. The M-CSFR/Stat3 signals might be potential targets for therapeutic inhibition of macrophage-related cell–cell interaction, an approach that may well prove promising for patients with high grade glioma.

Acknowledgments

We thank Ms Emi Kiyota, Mr Osamu Nakamura, and Ms Yui Hayashida (Department of Cell Pathology, Kumamoto University) for their technical assistance. This study was supported in part by Grants-in-Aid for Scientific Research (B20390113, 21790388) from the Ministry of Education, Culture, Sports, Science, and Technology of Japan.

Disclosure Statement

The authors have no conflict of interest.

References

1 Pollard JW. Tumour-educated macrophages promote tumour progression and metastasis. *Nat Rev Cancer* 2004; **4**: 71–8.
2 Sica A, Schioppa T, Mantovani A, Allavena P. Tumour-associated macrophages are a distinct M2 polarised population promoting tumour progression: potential targets of anti-cancer therapy. *Eur J Cancer* 2006; **42**: 717–27.
3 Gordon S. Alternative activation of macrophages. *Nat Rev Immunol* 2003; **3**: 23–35.
4 Jensen TO, Schmidt H, Moller HJ *et al.* Macrophage markers in serum and tumor have prognostic impact in American Joint Committee on Cancer stage I/II melanoma. *J Clin Oncol* 2009; **27**: 3330–7.
5 Espinosa I, Beck AH, Lee CH *et al.* Coordinate expression of colony-stimulating factor-1 and colony-stimulating factor-1-related proteins is associated with poor prognosis in gynecological and nongynecological leiomyosarcoma. *Am J Pathol* 2009; **174**: 2347–56.
6 Komohara Y, Ohnishi K, Kuratsu J, Takeya M. Possible involvement of the M2 anti-inflammatory macrophage phenotype in growth of human gliomas. *J Pathol* 2008; **216**: 15–24.
7 Kurahara H, Shinchi H, Mataki Y *et al.* Significance of M2-polarized tumor-associated macrophage in pancreatic cancer. *J Surg Res* 2009; **167**: e211–9.
8 Hasita H, Komohara Y, Okabe H *et al.* Significance of alternatively activated macrophages in patients with intrahepatic cholangiocarcinoma. *Cancer Sci* 2010; **101**: 1913–9.
9 Komohara Y, Hasita H, Ohnishi K *et al.* Macrophage infiltration and its prognostic relevance in clear cell renal cell carcinoma. *Cancer Sci* 2011; **102**: 1424–31.
10 Niino D, Komohara Y, Murayama T *et al.* Ratio of M2 macrophage expression is closely associated with poor prognosis for Angioimmunoblastic T-cell lymphoma (AITL). *Pathol Int* 2010; **60**: 278–83.
11 Steidl C, Lee T, Shah SP *et al.* Tumor-associated macrophages and survival in classic Hodgkin's lymphoma. *N Engl J Med* 2010; **362**: 875–85.

12 Nishie A, Ono M, Shono T *et al.* Macrophage infiltration and heme oxygenase-1 expression correlate with angiogenesis in human gliomas. *Clin Cancer Res* 1999; **5**: 1107–13.
13 Hirano H, Tanioka K, Yokoyama S, Akiyama S, Kuratsu J. Angiogenic effect of thymidine phosphorylase on macrophages in glioblastoma multiforme. *J Neurosurg* 2001; **95**: 89–95.
14 Hussain SF, Yang D, Suki D, Aldape K, Grimm E, Heimberger AB. The role of human glioma-infiltrating microglia/macrophages in mediating antitumor immune responses. *Neuro Oncol* 2006; **8**: 261–79.
15 Zhai H, Heppner FL, Tsirka SE. Microglia/macrophages promote glioma progression. *Glia* 2011; **59**: 472–85.
16 Yu H, Kortylewski M, Pardoll D. Crosstalk between cancer and immune cells: role of STAT3 in the tumour microenvironment. *Nat Rev Immunol* 2007; **7**: 41–51.
17 Yoshimura A. Signal transduction of inflammatory cytokines and tumor development. *Cancer Sci* 2006; **97**: 439–47.
18 Abou-Ghazal M, Yang DS, Qiao W *et al.* The incidence, correlation with tumor-infiltrating inflammation, and prognosis of phosphorylated STAT3 expression in human gliomas. *Clin Cancer Res* 2008; **14**: 8228–35.
19 Page BD, Ball DP, Gunning PT. Signal transducer and activator of transcription 3 inhibitors: a patent review. *Expert Opin Ther Pat* 2011; **21**: 65–83.
20 Cheng F, Wang HW, Cuenca A *et al.* A critical role for Stat3 signaling in immune tolerance. *Immunity* 2003; **19**: 425–36.
21 Wu L, Du H, Li Y, Qu P, Yan C. Signal transducer and activator of transcription 3 (Stat3C) promotes myeloid-derived suppressor cell expansion and immune suppression during lung tumorigenesis. *Am J Pathol* 2011; **179**: 2131–41.
22 Fujita M, Kohanbash G, Fellows-Mayle W *et al.* COX-2 blockade suppresses gliomagenesis by inhibiting myeloid-derived suppressor cells. *Cancer Res* 2011; **71**: 2664–74.
23 Hussain SF, Kong LY, Jordan J *et al.* A novel small molecule inhibitor of signal transducers and activators of transcription 3 reverses immune tolerance in malignant glioma patients. *Cancer Res* 2007; **67**: 9630–6.
24 Chihara T, Suzu S, Hassan R *et al.* IL-34 and M-CSF share the receptor Fms but are not identical in biological activity and signal activation. *Cell Death Differ* 2010; **17**: 1917–27.
25 Takaishi K, Komohara Y, Tashiro H *et al.* Involvement of M2-polarized macrophages in the ascites from advanced epithelial ovarian carcinoma in tumor progression via Stat3 activation. *Cancer Sci* 2010; **101**: 2128–36.
26 Horikawa T, Komohara Y, Kiyota E, Terasaki Y, Takagi K, Takeya M. Detection of guinea pig macrophages by a new CD68 monoclonal antibody, PM-1K. *J Mol Histol* 2006; **37**: 15–25.
27 Komohara Y, Horlad H, Ohnishi K *et al.* M2 macrophage/microglial cells induce activation of Stat3 in primary central nervous system lymphoma. *J Clin Exp Hematop* 2011; **51**: 93–9.
28 Sica A, Mantovani A. Macrophage plasticity and polarization: in vivo veritas. *J Clin Invest* 2012; **122**: 787–95.
29 Baay M, Brouwer A, Pauwels P, Peeters M, Lardon F. Tumor cells and tumor-associated macrophages: secreted proteins as potential targets for therapy. *Clin Dev Immunol* 2011; **2011**: 565187.
30 Zheng Y, Cai Z, Wang S *et al.* Macrophages are an abundant component of myeloma microenvironment and protect myeloma cells from chemotherapy drug-induced apoptosis. *Blood* 2009; **114**: 3625–8.
31 Zhang L, Alizadeh D, Van Handel M, Kortylewski M, Yu H, Badie B. Stat3 inhibition activates tumor macrophages and abrogates glioma growth in mice. *Glia* 2009; **57**: 1458–67.
32 Fujita M, Zhu X, Sasaki K *et al.* Inhibition of STAT3 promotes the efficacy of adoptive transfer therapy using type-1 CTLs by modulation of the immunological microenvironment in a murine intracranial glioma. *J Immunol* 2008; **180**: 2089–98.
33 Douglass TG, Driggers L, Zhang JG *et al.* Macrophage colony stimulating factor: not just for macrophages anymore! A gateway into complex biologies. *Int Immunopharmacol* 2008; **8**: 1354–76.
34 Stein J, Borzillo GV, Rettenmier CW. Direct stimulation of cells expressing receptors for macrophage colony-stimulating factor (CSF-1) by a plasma membrane-bound precursor of human CSF-1. *Blood* 1990; **76**: 1308–14.
35 Novak U, Harpur AG, Paradiso L *et al.* Colony-stimulating factor 1-induced STAT1 and STAT3 activation is accompanied by phosphorylation of Tyk2 in macrophages and Tyk2 and JAK1 in fibroblasts. *Blood* 1995; **86**: 2948–56.
36 Sherry MM, Reeves A, Wu JK, Cochran BH. STAT3 is required for proliferation and maintenance of multipotency in glioblastoma stem cells. *Stem Cells* 2009; **27**: 2383–92.
37 Wu A, Wei J, Kong LY *et al.* Glioma cancer stem cells induce immunosuppressive macrophages/microglia. *Neuro Oncol* 2010; **12**: 1113–25.
38 Kubota Y, Takubo K, Shimizu T *et al.* M-CSF inhibition selectively targets pathological angiogenesis and lymphangiogenesis. *J Exp Med* 2009; **206**: 1089–102.
39 Priceman SJ, Sung JL, Shaposhnik Z *et al.* Targeting distinct tumor-infiltrating myeloid cells by inhibiting CSF-1 receptor: combating tumor evasion of antiangiogenic therapy. *Blood* 2010; **115**: 1461–71.
40 Coniglio SJ, Eugenin E, Dobrenis K *et al.* Microglial stimulation of glioblastoma invasion involves EGFR and CSF-1R signaling. *Mol Med* 2012; **18**: 519–27.

doi: 10.1111/cas.12015

J Neurooncol (2012) 109:399–404
DOI 10.1007/s11060-012-0907-3

CLINICAL STUDY

Fatty acid synthase is a predictive marker for aggressiveness in meningiomas

Keishi Makino · Hideo Nakamura · Taku-ichiro Hide · Shigetoshi Yano · Jun-ichiro Kuroda · Ken-ichi Iyama · Jun-ichi Kuratsu

Received: 29 February 2012 / Accepted: 29 May 2012 / Published online: 29 June 2012

Abstract Meningiomas are the most frequent intracranial tumors. Although most are benign WHO grade I tumors, grade II and III tumors are aggressive and survival is poor. Treatment options for grade II and III meningiomas are limited, and molecular targets are few. The re-programming of metabolic pathways including glycolysis, lipogenesis, and nucleotide synthesis is a hallmark of the physiological changes in cancer cells. Because fatty acid synthase (FAS), the enzyme responsible for the de-novo synthesis of fatty acids, has emerged as a potential therapeutic target for several cancers, we investigated its involvement in meningiomas. We subjected 92 paraffin-embedded samples from 57 patients with grade I, 18 with grade II and III, and six with radiation-induced tumors to immunohistochemical study of FAS. Whereas its expression was increased in grade II and III meningiomas (62.9 %) compared with grade I tumors (29.8 %) (chi-squared test: $p < 0.001$), FAS was expressed in grade I tumors with a high MIB-1 index and infiltration into surrounded tissues. All radiation-induced meningiomas expressed FAS and its expression was positively correlated with the MIB-1 index ($p < 0.005$). Our findings suggest that increased FAS expression reflects the aggressiveness of meningiomas and that it may be a novel therapeutic target for treatment of unresectable or malignant tumors.

K. Makino (✉) · H. Nakamura · T. Hide · S. Yano · J. Kuroda · J. Kuratsu
Department of Neurosurgery, Faculty of Medicine, Kumamoto University, 1-1-1 Honjo, Kumamoto 860-8556, Japan
e-mail: kmakino@fc.kuh.kumamoto-u.ac.jp

K. Iyama
Department of Surgical Pathology, Kumamoto University Hospital, Kumamoto, Japan

Keywords Meningioma · Fatty acid synthesis · Immunohistochemistry · Radiation-induced

Introduction

Meningiomas are among the most frequent tumors of the central nervous system; they account for 30–35 % of these tumors [1, 2] Although most meningiomas are regarded as benign (WHO grade I), approximately 20 % are atypical (WHO grade II) or anaplastic (WHO grade III) and considerably more aggressive, and thus associated with higher morbidity and mortality. Treatment options for high-grade meningiomas are limited, and few biologically-based targets have been identified.

Genetic studies identified several genes associated with the pathogenesis of meningioma. Inactivating mutations in the neurofibromatosis type 2 gene (NF2) were present in most sporadic meningiomas [3]. Loss of heterozygosity at chromosomes 22q, 1p, 14q, 6q, and 10 has been investigated [4, 5]. Atypical and anaplastic meningiomas manifest changes involving the CDKN2A, p14, and CDKN2B tumor suppressor genes [6], and expression of the progesterone receptor is inversely related to the malignancy grade [7]. Ionizing radiation is a known risk factor for the development of meningioma. Although radiation-induced meningiomas morphologically resemble sporadically-arising tumors, they are often aggressive and have malignant behavior, for example multiplicity and higher post-treatment recurrence [8, 9]. In radiation-induced meningiomas NF2 mutations and loss on chromosome 22 may be seen less often whereas loss on chromosome 1p may be common [10, 11]. These genes and molecules provide important insights into the formation and progression of meningiomas, however, no new targets for their treatment have been identified.

Fatty acid synthase (FAS), a 270-kDa cytosolic multifunctional polypeptide, is the primary enzyme required for catalyzing the conversion of dietary carbohydrates to fatty acids (enzyme commission number; 2.3.1.85). Expression of FAS is relatively low in normal cells; in human cancers, including breast, thyroid, colon, ovary, lung, and prostate cancer, on the other hand, it is expressed at significantly higher levels [12–19]. Moreover, high levels of FAS expression have been reported in WHO grade II and III meningiomas [20]. FAS expression levels have been shown to correlate with tumor progression, aggressiveness, and metastasis [15, 16]. As FAS is strongly linked to tumor cell proliferation [15] and is preferentially expressed in cancer cells, it is an attractive target for novel anticancer therapy [16, 19]. Here we investigated the expression of FAS in sporadic and radiation-induced meningiomas.

Materials and methods

Tumor samples

We performed immunohistochemical analysis of 92 paraffin-embedded samples from 81 meningioma patients. Of these, 57 had WHO grade I tumors (meningothelial, $n = 36$, transitional, $n = 6$; fibrous, $n = 6$; microcystic, $n = 4$; angiomatous, $n = 3$; secretory, $n = 1$; metaplastic, $n = 1$). Grade II tumors were found in 17 patients (atypical, $n = 15$; clear cell, $n = 2$); one patient presented with a grade III anaplastic tumor. The other six patients had radiation-induced meningiomas (meningothelial, $n = 4$; atypical, $n = 2$).

Immunohistochemistry

We used our previously-described immunohistochemistry procedure [21]. After routine deparaffinization, rehydration, and blocking of endogenous peroxidase activity we performed microwave-enhanced antigen retrieval. Slide-mounted sections immersed in 0.01 M sodium citrate buffer (pH 6.0) were placed for 15 min in a 700-W microwave oven at maximum power. FAS immunostaining was with anti-FAS antibody (1:50; Santa Cruz Biotechnology). To assess the intensity of immunoexpression, an intensity distribution score was recorded by optical analysis using the staining intensity of 50 % of positive cells (0: none; 1: weak, 2: moderate, 3: strong). The scores were determined by concordance among the scores of two independent reviewers unaware of the clinico-pathological data. For statistical analysis, 0 and 1 were defined as negative, and 2 and 3 as positive expression. For negative controls the primary antibody was substituted with normal rabbit IgG. Anti-MIB-1 antibody (1:50) was from Dako.

Statistical analysis

Differences between expression of FAS among the histologic meningioma tumor types were evaluated by use of the chi-squared test. Differences of $p < 0.05$ were regarded as statistically significant. Statistical analysis was with StatMate III software (version III for Macintosh; Atoma, Tokyo, Japan). The correlation between FAS expression and the MIB-1 index was analyzed for a Spearman rank order correlation (assuming non-Gaussian data distribution) by use of GraphPad Prism software (GraphPad Software, San Diego, USA). Differences were considered significant at $p < 0.05$. Recurrence or regrowth-free survival was assessed by the Kaplan–Meier method with the date of primary surgery as the entry date. The end point for recurrence or regrowth-free survival analysis was detection of tumor recurrence or regrowth. The Mantel–Cox log-rank test was used to assess the strength of the association between the recurrence or regrowth-free interval; single variables were patient age and gender, the presence of peritumoral edema, infiltration into surrounding tissues, the MIB-1 index, and the extent of FAS expression by the tumor.

Results

We investigated FAS immunoexpression in 92 human meningioma samples. Whereas in benign (WHO grade I) tumors FAS expression tended to be absent or weak, in aggressive meningiomas (WHO grades II and III, and radiation-induced tumors) it was moderate or strong (Table 1). In 26 of 57 grade I tumors (45.6 %) FAS expression was negative (Fig. 1a); this was true in six of 27 (22.2 %) grade II or III meningiomas. For all eight radiation-induced tumors FAS expression was moderate or strong (Fig. 2). The difference between grade I and the other meningiomas was statistically significant (chi-squared test $p < 0.001$). Among grade I tumors, those with infiltration into surrounding tissues, for example the temporal or parietal bone and muscles expressed FAS (Fig. 1b, c), as did WHO grade II clear-cell and atypical meningiomas (Fig. 1d, e).

To investigate the correlation between FAS expression and clinico-pathological factors we performed statistical

Table 1 FAS expression in 92 meningioma samples

	0 (None)	1 (Weak)	2 (Moderate)	3 (Strong)
Grade I	26	14	12	5
Grade II and III	6	4	10	7
Radiation-induced	0	0	7	1

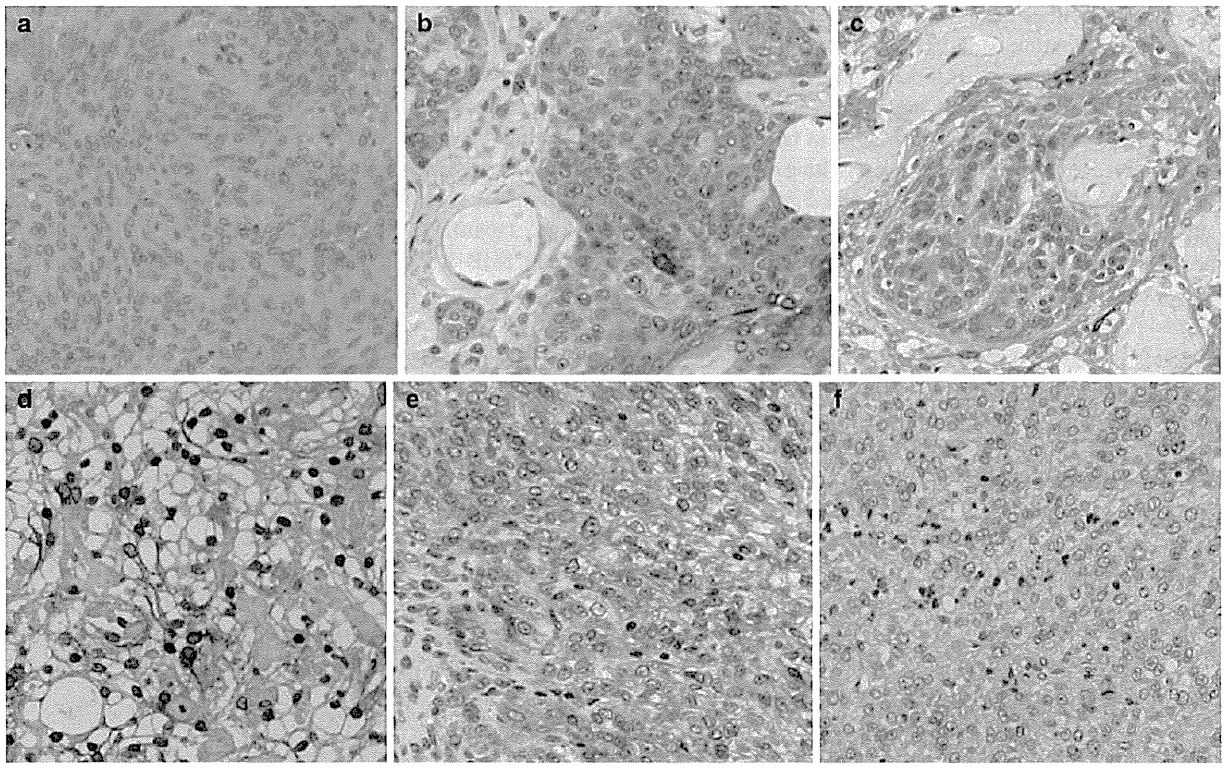

Fig. 1 FAS immunostaining of neoplastic cells (original magnification, ×200). **a** No FAS expression in a meningothelial meningioma (WHO grade I) (**b–e**) FAS expression in a meningothelial meningioma with infiltration into temporal bone and muscles (**b**), an angiomatous meningioma with infiltration into parietal bone (**c**), a clear cell meningioma (**d**), and an atypical meningioma (**e**), and its substitution with normal IgG on same specimen of atypical meningioma (**f**)

analysis. We found significant associations between FAS expression and a high histological tumor grade ($p = 0.047$), infiltration into surrounding tissues ($p = 0.011$), and MIB-1 index (≥5 %, $p = 0.001$) (Table 2). Among 57 grade I tumors, infiltration was identified in 26 cases. In 12 of 26 infiltrating tumors (46.2 %), FAS expression was positive. On the other hand, 5 of 31 tumors (16.1 %) without infiltration were positive. There was statistical difference between with and without infiltration ($p = 0.014$).

Spearman rank order correlation also confirmed a significant association between FAS expression and a high MIB-1 index ($p = 0.0012$) (Fig. 3). Of the 57 patients with WHO grade I meningiomas, 11 underwent Simpson grade I resection; for 23 it was Simpson grade II, for one Simpson grade III, and 22 were treated by Simpson grade IV resection. During 1–109 month follow up (median 20.8 months), 10 of the 57 patients developed tumor recurrence or regrowth; nine of these patients had undergone Simpson grade IV resection. During a median follow-up of 28.6 months, 39.1 % of patients who were treated by Simpson grade III or IV resection manifested tumor progression. Univariate analysis showed that infiltration into surrounding tissues and a MIB-1 index higher than 5 % were significant prognostic factors for the development of recurrence or regrowth (Table 3). As shown in Fig. 4 there was no significant difference between the disease-free survival of meningioma patients that did or did not express FAS ($p = 0.2761$).

Discussion

On the basis of clinical and pathologic findings, most meningiomas are benign, although predicting the behavior of individual meningiomas remains difficult. Even grade I meningiomas can manifest clinically aggressive behavior, for example penetration of the arachnoidal border and destruction of the bone. Residual tumors may regrow rapidly and totally resected tumors can recur [22–26]. As recurrence may have the most significant impact on patient survival and quality of life, it may be the most important component of the definition of clinical aggressiveness. Immunohistologically, the MIB-1 index [27], progesterone receptor [28, 29], and vascular endothelial growth factor [30, 31] may make it possible to evaluate the aggressive potential of meningiomas. We found that a high MIB-1